공학석사 학위논문

Evaluation of Equivalent Linear Methods for Seismic Response Analysis of Base Isolated Structures

면진 구조물 응답 해석을 통한

등가선형 방법의 평가

2017 년 2 월

서울대학교 대학원

건축학과

김 서 연

Evaluation of Equivalent Linear Methods for Seismic Response Analysis of Base Isolated Structures

지도 교수 이 철 호

이 논문을 공학석사 학위논문으로 제출함
2017 년 2 월

서울대학교 대학원
건축학과
김 서 연

김서연의 공학석사 학위논문을 인준함
2017 년 2 월

위 원 장 _____ (인)

부위원장 _____ (인)

위 원 _____ (인)

Abstract

Evaluation of Equivalent Linear Methods for Seismic Response Analysis of Base Isolated Structures

Kim, Seo Yeon
Department of Architecture and Architectural Engineering
College of Engineering
Seoul National University

Base isolation system protects structures against severe earthquakes by inserting isolators with low lateral stiffness between supporting points and superstructure so that most of deformation occurs at isolators. In the design of base isolation system, idealized bilinear models have been generally used to represent the hysteretic behavior of isolators such as high damping rubber, lead-rubber bearings and friction pendulum. In various design standards and codes including IBC 2015, FEMA-440 and Eurocode 8, equivalent linear (EL) methods using equivalent viscous damping and equivalent stiffness are permitted for seismically isolated structures when specific conditions are met.

In this study, estimation accuracy of five existing EL models are evaluated

for the multi-degree-of-freedom structure isolated with lead-rubber bearings. Analyses including wide range of ductility ratio were carried out by considering post-to-yield stiffness ratio and isolated period as variables. Earthquake data consist of 20 sets of recorded or simulated data provided from FEMA. Relative displacement of the base floor and absolute acceleration of roof floor are the main indexes of the structure response.

The result indicates that several EL methods estimate the relative displacement of base floor almost accurately with error ratio less than 5 percent. Relative displacement is the index that affects the structural damage, so that EL method is quite reliable method for the design in the aspect of the isolators' performance. On the other hand, EL method significantly underestimates the response of the absolute acceleration which can affect the damage of the non-structural member and equipment inside of the structure. It is demonstrated that modified EL method includes structure mode is required in further researches.

Keywords : Base isolation, Nonlinear dynamic analysis, Equivalent linear analysis, Lead rubber bearings, Structure response

Student Number : 2015-21097

Contents

List of Tables

List of Figures

List of Symbols

c	damping coefficient
M	total mass of the superstructure
m	floor mass
E_D	hysteretic energy dissipated per cycle of motion through inelastic deformation
E_{S0}	elastic strain energy based upon secant stiffness
f_y	yield strength
f_u	ultimate strength
k_{eq}	equivalent stiffness
k_i	initial elastic stiffness
k_p	post yield stiffness
Q_y	normalized yield strength
T_f	natural period of the fixed base structure
T_b	natural period of the base isolated structure
T_0	initial period of seismic isolation system
T_p	target period of base isolated structure
u_y	yield displacement
u_0	ultimate displacement

Greek letters

α	post-to-pre yield stiffness ratio ($\alpha = k_p / k_i$)
μ	ductility ratio ($\mu = u_0 / u_y$)
ξ_0	inherent viscous damping ratio
ξ_{eq}	equivalent damping ratio
ξ_f	damping ratio of the fixed base structure
ξ_{hyst}	damping ratio by hysteretic behavior
ξ_b	damping ratio of the base isolated structure
ω_f	natural frequency of the fixed base structure
ω_b	natural frequency of the base isolated structure

Chapter 1. Introduction

1.1 Concept of Base Isolation

As severe damages are caused by earthquakes, there have been various researches to protect the buildings and facilities against earthquakes. Base isolation, also known as seismic isolation, is one of the most effective methods to mitigate seismic risk. A variety of building and bridge structures have been constructed around the world using base isolation since the early 1970's, particularly during the 1980s and 1990s.

Base isolation system protects the structure by installing isolator, which has much lower lateral stiffness than lateral stiffness of superstructure between foundation and superstructure. Because of the lower stiffness, isolator has flexible behavior and decouples the ground motions and superstructure motions so that reduces the earthquake damage which is transferred to superstructure and equipment inside the building.

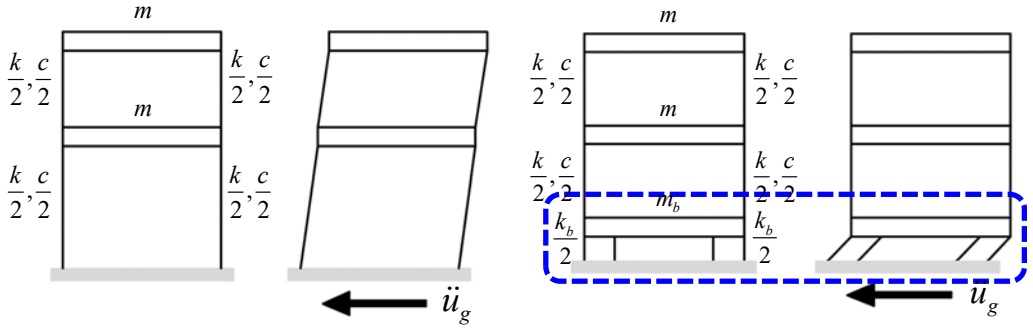

(a) Fixed base building (b) Base isolated building

Figure 1.1 Behaviors in a fixed base and base isolated structure

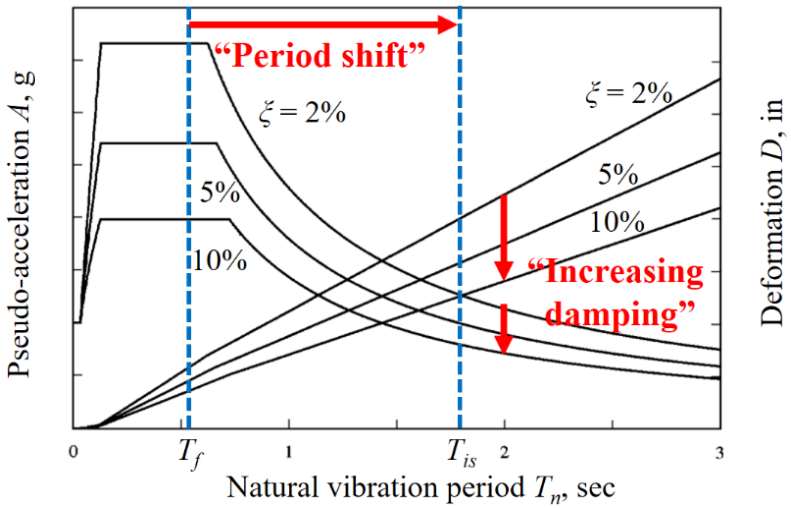

Figure 1.2 Period shift of base isolation

There are mainly two advantageous effects of base isolation. First one is the reduction of lateral force in the superstructure. As previously stated, isolator behaves flexibly, therefore the fundamental period of the structure is lengthened (period shift) beyond the most predominant period of typical earthquakes. That means the natural period of the structure is shifted from T_f(fixed base condition) to T_{is} (base isolated condition) in Figure 1.2. In addition, isolator adds damping which dissipates the residual input energy and limits the force transmitted to the structure. These lead the reduction of the acceleration response of structure and consequently the lateral forces in the structure. Second one is the concentration of lateral displacements at the isolation interface or modification of the mode shape. The magnitude of interstory drift depends on the combination of the first several predominant modes of the vibration of the structure and it can cause both structural and non-structural damage. For fixed base structure, lateral seismic displacements are distributed over the height of

the structure so there's considerable interstory drift. On the other hand, for isolated structure, the predominant mode of vibration is related to displacement of the isolation system. The superstructure above the isolation system moves almost like rigid body, and interstory drift within the superstructure is significantly reduced. It means that the isolation system concentrates most of lateral displacements at the isolation interface and that will be the predominant mode shape of the isolated structure.

1.2 General Properties of Base Isolated Structures

This chapter includes contents about how the dynamics of multistory building is modified by base isolation system. In the Figure 1.3 (a), the *N*-story building on a fixed system is defined with the mass matrix m_f, damping matrix c_f, and stiffness matrix k_f; where the subscript *f* denotes "fixed base". If the mass of the structure is idealized as lumped at the floor levels, m_f can be expressed as diagonal matrix with diagonal element m_i, the mass lumped at the i^{th} floor. The total mass of the building is M ($=\sum m_i$). The natural periods and modes of vibration of the fixed-base system are denoted by T_{if} and ϕ_{if} respectively, where i = 1, 2, …, N. For the fixed-base system, properties of the structure are

$$\omega_f = \sqrt{\frac{k_f}{m_f}} \quad T_f = \frac{2\pi}{\omega_f} \quad \xi_f = \frac{c_f}{2m_f\omega_f} \tag{1-1}$$

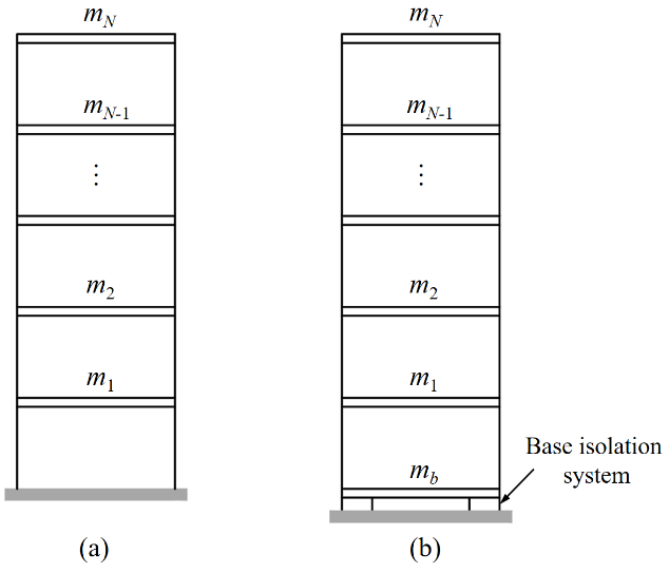

Figure 1.3 (a) Fixed-base *N*-story building; (b) isolated *N*-story building

Figure 1.3 (b) illustrates the *N*-story building supported on a base isolation system including base slab of mass m_b. With the characteristics of the isolation system denoted as lateral stiffness k_b and damping c_b, two properties of isolation system are expressed as

$$\omega_b = \sqrt{\frac{k_b}{M + m_b}} \quad T_b = \frac{2\pi}{\omega_b} \quad \xi_b = \frac{c_b}{2(M + m_b)\omega_b} \tag{1-2}$$

where T_b means the natural vibration period and ξ_b the damping ratio of the isolation system with the building assumed to be rigid.

1.3 Typical Types of Base Isolators

1.3.1 Friction pendulum

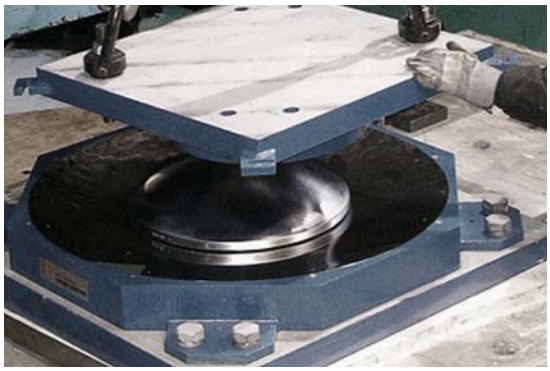

Figure 1.4 Friction pendulum system (MAURER)

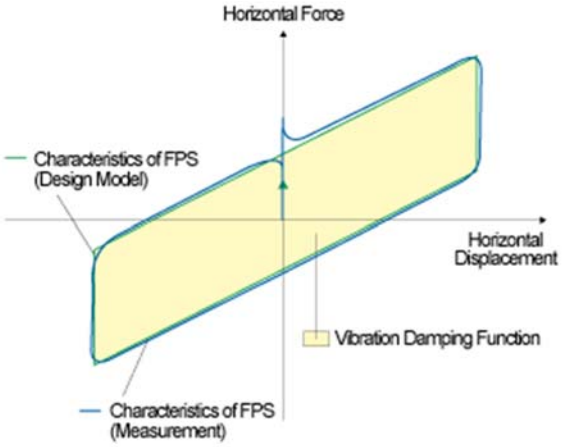

Figure 1.5 Period shift of base isolation

Friction pendulum is a friction-type sliding bearing that uses gravity as the restoring force. As Figure 1.4, the friction pendulum isolator consists of polished stainless steel spherical concave surface, an articulated slider, and a low friction composite liner. The side of the articulated slider in contact with the spherical surface is coated with a low-friction composite material. When earthquake occurs the articulated slider travels on a spherical concave lining

surface so that earthquake energy is dissipated and superstructure moves in a pendulum motion. This sliding system also has self-centering feature because of the concave shape of the surface.

Hysteretic behavior is shown in Figure 1.5. The period of oscillation is a function of the radius of the concave surface and is independent of the mass of the superstructure. Damping is provided by the dynamic friction force, which can be varied by adjusting the properties of the low friction composite liner material. Typical damping values are between 10 to 30% of critical. The effective stiffness of the friction pendulum system is dependent on the friction coefficient of the system and the maximum displacement of the isolator.

1.3.2 Laminated-rubber bearings

As shown in Figure 1.7, laminated-rubber bearings consist of elastomeric rubber layers alternating with steel plates solidly joined together under high pressure and temperature through vulcanization. The steel plates provide enhanced vertical stiffness and confinement so they impede the bulging deformation of the compressed rubber. So, laminated-rubber bearings can withstand large gravity loads, while providing only a fraction of the lateral stiffness of the superstructure.

Figure 1.6 shows hysteretic behavior of laminated rubber bearing. It behaves almost linearly with low damping of the order of 5% to 10%. and lateral stiffness of the laminated rubber bearing is relatively low as pure shear deformations occur in the rubber only.

Damping of the laminated rubber bearing can be modelled by equivalent viscous damping. Experiments have shown that the energy dissipation through

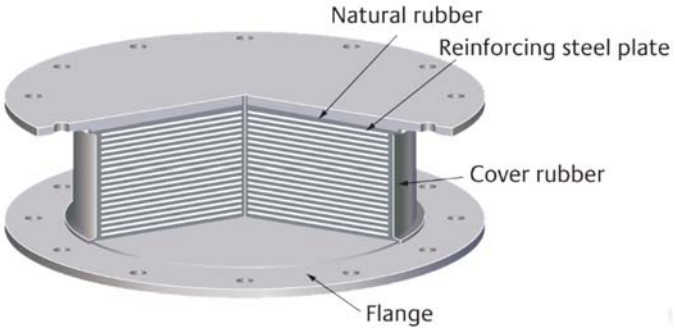

Figure 1.7 Schematic of laminated-rubber bearing

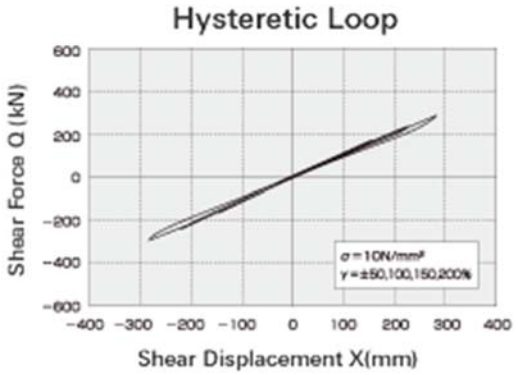

Figure 1.6 Hysteresis loop of laminated-rubber bearing

shear deformations in rubber layers of laminated-rubber bearings is proportional to velocity. Therefore, damping in laminated-rubber bearings can be modelled by equivalent viscous damping. Typical laminated rubber bearings can be modelled by damping of the order of 5% to 10%.

However, laminated-rubber bearings have some disadvantages. One is the relatively low damping caused by the rubber. There have been various efforts to develop the laminated-rubber bearings with high damping rubbers and theses kind of devices have been used in Japan. High damping rubber provided evidently improved energy dissipation performance to the laminated-rubber bearings than laminated-rubber bearings with low damping rubber reaching values of equivalent viscous damping of approximately 20% at shear strains of

300%. Despite the improvement of energy dissipation capacity, high damping rubber was not selected as primary alternative because of the critical problems. High damping rubber is more vulnerable to the heat so the property changes during cyclic loading and to aging effects influencing stiffness and energy dissipation capacity. Furthermore, supplemental damping can be provided to a system isolated with laminated-rubber bearings through external supplemental damping devices such as hysteretic or viscous dampers.

Another disadvantage of laminated-rubber bearings is the low initial lateral stiffness. The steel plate vulcanized to the rubber layer limits severely the flexural deformations of a laminated-rubber bearing. Therefore, it can be assumed that pure shear deformations occur in the rubber only. It can be shown in the hysteresis loop of laminated-rubber bearings above Figure 1.6. If the initial stiffness is too low, isolator can be activated so easily with the wind load or other typical lateral load that is not critical.

1.3.3 Lead-rubber bearings

The lead-rubber bearing is a variant of laminated-rubber bearing that contains cylindrical lead plug inserted in the center of device, as shown in Figure 1.9. The lead plug increases the damping by hysteretic shear deformations therefore, separate damper is not required generally.

There are some reasons why lead is appropriate as the material for the core plug. The main reason is that it has advantage in its behavior. Lead behaves approximately as an elastic-plastic solid, at room temperature, and yields in shear at relatively low stress of about 10 MPa providing the bearing with a bilinear response. Moreover, unlike mild steel, lead recrystallizes at normal temperature, so that repeated yielding does not cause fatigue failure and

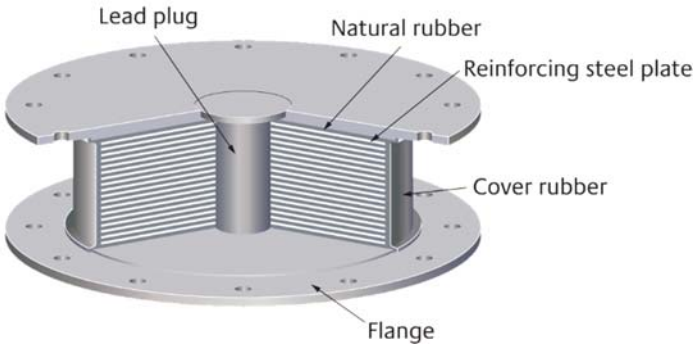

Figure 1.9 Schematic of lead-rubber bearings

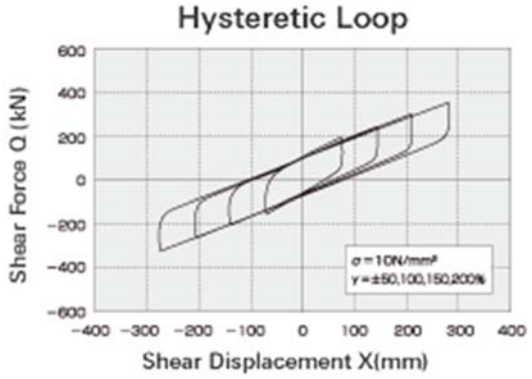

Figure 1.8 Hysteresis loop of lead-rubber bearings

properties of lead are continuously restored when cycled in the inelastic range. Lastly, it is commonly available material that used at a purity level of more than 99.9%.

Figure 1.8 indicates the hysteretic behavior of lead-rubber bearings and in the response, it can be found that before yielding, the lateral stiffness is much larger since not only the rubber but also the lead deforms elastically. On the other hand, after yielding of the lead plug, the lateral stiffness is decreased to the elastic shear stiffness of the rubber only. So the isolator behaves flexibly and dissipates the earthquake energy effectively.

In this study, lead-rubber bearing is mainly discussed as standard isolator considering practical aspect.

1.4 Objectives and Scope

As mentioned above, base isolation system is the effective way to mitigate the damage of the structure from the earthquake excitations. To adjust the base isolation system with simple process, some methods have been devised. First, isolators which have relatively low stiffness is inserted between the superstructure and foundation so the deformation occurred through the earthquake is concentrated in the isolator mostly that superstructure is considered as rigid element. So there were various researches that analyzed the behavior of structures characterized by single-degree-of-freedom. Second, the hysteresis of base isolator is nonlinear shape with the high stiffness before the yield and low stiffness after the yield of the isolator. However, as the analysis of the nonlinear takes excessive time and effort, many design codes and criteria such as IBC 2015, FEMA-440 and Eurocode 8, equivalent linear (EL) methods using equivalent viscous damping and equivalent stiffness are permitted for seismically isolated structures when specific conditions are met.

In this study, estimation accuracy of existing EL methods was evaluated for the base isolated structure characterized by the multi-degree-of-freedom (MDOF). For the analysis, previous research review was done with five advanced EL methods. After that, the responses of the 6 degree-of-freedom system were analyzed by nonlinear and equivalent linear method. From the analysis comparison, the estimation accuracy of the EL methods were evaluated and the aspects of the floor responses were analyzed. The indicators are selected as relative displacement of the isolator and absolute acceleration of the roof floor to figure out the damage of the structural and non-structural member that affect the performance of the structure. Furthermore, different from the

advanced researches were considered only about the peak value of the responses, this study includes time history analysis was carried out to examine the structure behavior through whole time.

Chapter 2. Hysteretic Behavior of Base Isolator

2.1 Nonlinear Hysteretic Behavior of Isolator

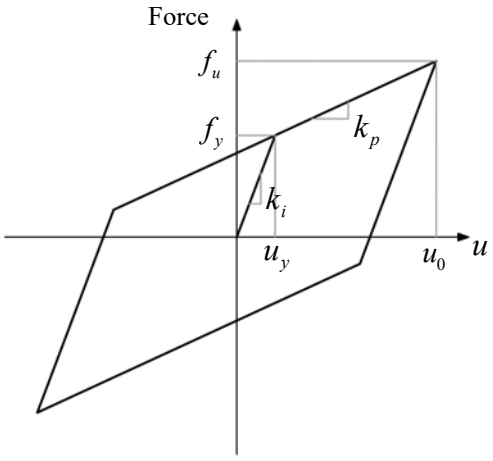

Figure 2.1 Idealized bilinear hysteresis model of LRBs

Isolators behave nonlinearly through complicated hysteresis but in the design of isolation system, the hysteresis of isolator is approximated as bilinear systems which can be represented by parallelogram-shaped force-displacement hysteresis loop shown in Figure 2.1. Isolator initially moves with high lateral stiffness k_i and yields at relatively low displacement, then moves flexibly with low lateral stiffness k_p. The area of the loop means dissipated energy.

The equation of motion under earthquake excitation of bilinear hysteretic behavior is expressed as

$$m\ddot{u} + c\dot{u} + f\left(u,\dot{u}\right) = -m\ddot{u}_g \tag{2-1}$$

where $\ddot{u}$, $\dot{u}$, and u indicate the acceleration, velocity, and displacement respectively. m is the mass matrix of the system, c is the damping coefficient matrix, $f(u,\dot{u})$ is the restoring force matrix, and $\ddot{u}_g$ is the ground acceleration.

2.2 Equivalent Linearization of Nonlinear Hysteresis

Nowadays, nonlinear systems can be solved easily through nonlinear time history analysis method as computer performance has been improved. However, solving of systems with a large quantity of degrees of freedom may require an excessive amount of time and effort when time history analysis methods are used. Also, the enormous amount of output results from such systems may be so detailed that it is impractical for engineers to sort out which data to use. Moreover, the number of different loading cases needed to be solved may be quite large. Thus, there will always be a need for good approximate methods of analysis of nonlinear systems.

Equivalent linearization (EL) method is one of the best known approximation methods. As expressed in Figure 2.2, the concept of this method is to transpose the nonlinear force to an equivalent linear behavior by using a fictitious viscous damping and shear stiffness which makes isolation system can reach approximately equal maximum displacement with nonlinear behavior. Therefore, replacing the bilinear system with a linear viscous damped system, the equation of motion may be expressed as

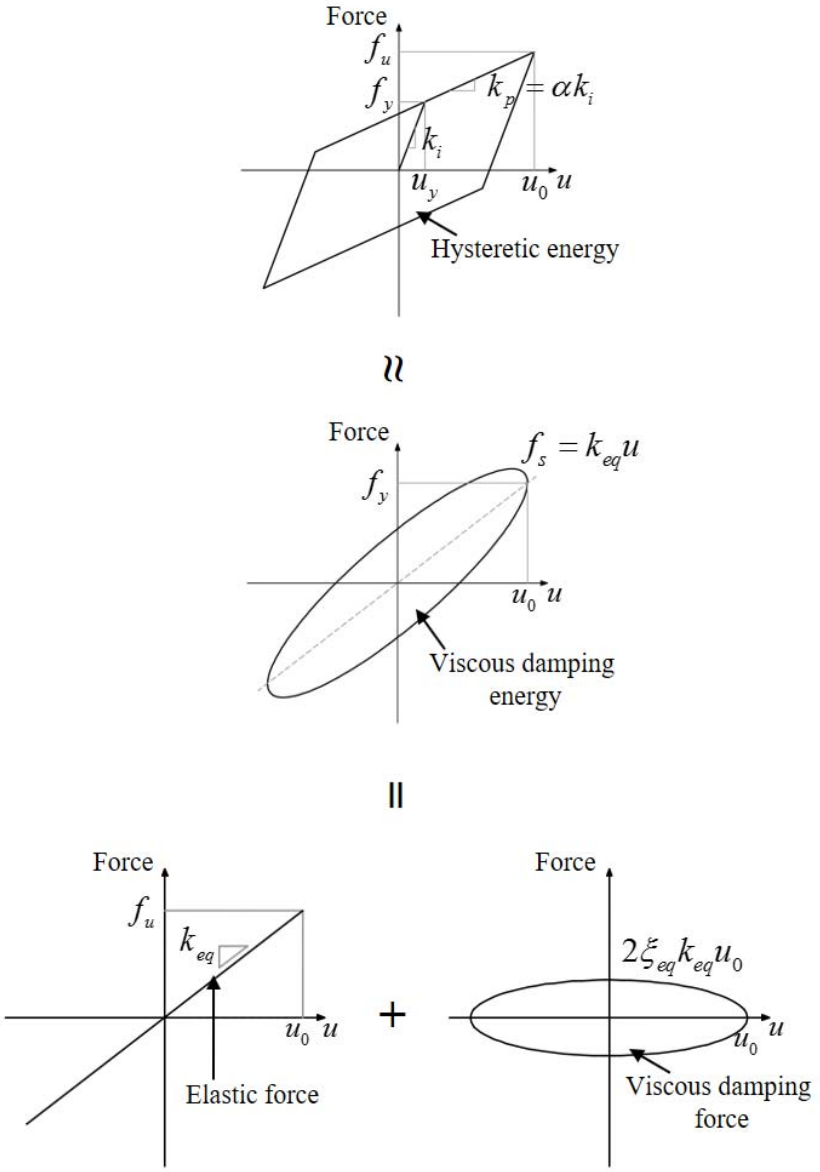

Figure 2.2 Equivalent linearization of bilinear hysteretic behavior

$$m\ddot{u}_{eq} + c_{eq}\dot{u}_{eq} + k_{eq}u_{eq} = -m\ddot{u}_g \tag{2-2}$$

where $\ddot{u}_{eq}$, $\dot{u}_{eq}$, and u_{eq} are the acceleration, velocity, and displacement of equivalent system respectively. m is the mass matrix of the system, c_{eq} is the equivalent damping coefficient matrix, k_{eq} is the equivalent lateral stiffness matrix, and $\ddot{u}_g$ is the ground acceleration. When initial damping is negligible, the error of equivalent linear method compared to nonlinear method is $f(u,\dot{u}) - c_{eq}\dot{u}_{eq} - k_{eq}u_{eq}$.

Most of design specifications such as IBC2015, FEMA-440, and Eurocode8 allow not only nonlinear method but also equivalent linear analysis method. EL methods can be used as the only design method for specific cases; for example, mid-to-low building that lies on firm ground and has short natural period etc. It also used for establishing level for the design displacements and forces or preliminary design when dynamic analysis is required.

2.3 Equivalent Linear (EL) Methods

Table 2.1 includes equivalent linear methods which have been proposed by various researchers. Among these, methods for base isolation is marked with color and methods are arranged in chronological order for each category. Each EL method considered different hysteretic behavior of isolator not only bilinear behavior but also Takeda model, stiffness degrading, pinching, etc.

Equivalent viscous damping ζ_{eq} and equivalent lateral stiffness k_{eq} is generally expressed with two parameters; post-to-pre yield stiffness ratio α (=k_p / k_i) and displacement ductility ratio μ (= u_0 / u_y) (Figure 2.2). In the right side

of the table, the variables of isolators' properties, post-to-pre yield stiffness ratio α and ductility ratio μ, considered for each EL methods are arranged. When the base isolation system is adopted, considerable deformation can occur even after the yielding of isolator. So among these values, EL methods with considering ductility ratio μ value under 8 is not sufficient for base isolation system and further study has to be made to adopt that kind of EL method.

Among them, 5 methods were chosen for this study. 5 methods can be classified to two groups by the manner to derive equivalent stiffness; EL methods base upon secant stiffness concept and EL methods base upon empirical formulas.

Table 2.1 Summary of existing EL methods

EL methods	Hysteresis type	α	μ
R&H (1964)	Bilinear	$0.00 \le \alpha \le 1.00$	$1 < \mu$
G&S (1974)	Takeda without hardening	$\alpha = 0.00$	$1 < \mu$
ASE (1979)	Bilinear	$0.00 \le \alpha \le 1.00$	$1 < \mu$
Iwan (1980)	Elastic-perfectly plastic	$\alpha = 0.00$	$1 < \mu \le 8$
JPWRI (1992)	Bilinear	$0.00 \le \alpha \le 1.00$	$1 < \mu$
Kow (1994)	Takeda with post-yield hardening	$\alpha = 0.05$	$1 < \mu$
ASD (1998)	Bilinear	$0.00 \le \alpha \le 1.00$	$1 < \mu$
K&B (2003)	Elastic-perfectly plastic, slightly degrading, moderately degrading, slip, origin-oriented, bilinear elastic	-	$2 \le \mu \le 8$
H&S (1993)	Bilinear	$\alpha = 0.05$	$1 < \mu \le 8$
H&C (1996)	Bilinear	$\alpha = 0.15$	$2 \le \mu \le 50$
G&I (2004)	Bilinear, stiffness degrading, strength and stiffness degrading, pinching	-	$1.25 \le \mu \le 10$
J&C (2006)	Bilinear	$0.05 \le \alpha \le 0.15$	$1 \le \mu \le 40$
D&B (2007)	Bilinear	$0.01 \le \alpha \le 0.2$	$2 \le A_pW/Q_y \le 10$*
J&O (2012)	Bilinear	$0.05 \le \alpha \le 0.15$	$1 < \mu \le 30$
L&Z (2015)	Bilinear	$0.02 \le \alpha \le 0.20$	$2 \le \mu \le 50$

* Note : Ap : the peak ground acceleration, W : the weight acting on isolator, Q_y: the characteristic strength

2.3.1 EL methods base upon secant stiffness concept

The first group of equivalent methods consists of EL methods base upon secant stiffness concept. EL methods proposed by Rosenblueth and Herrera, Dicleli and Buddaram, and Liu and Zordan were considered in this paper. For the sake of brevity, the methods above are abbreviated to R&H, D&B, and L&Z.

Rosenblueth and Herrera

Rosenblueth and Herrera firstly proposed the secant stiffness at maximum deformation as the basis for selecting the period ratio, as presented Figure 2.3. To determine the equivalent lateral stiffness, experiment under nonlinear cyclic loading test should be carried out in advance. The period ratio is derived with the equivalent stiffness which is the gradient of the line that connects the maximum displacement amplitude u_0 derived from the test and the starting point. With parameters, period ratio of the EL systems is given as

$$T_{eq} / T_0 = \sqrt{k_i / k_{eq}} = \sqrt{\mu / [1 + \alpha(\mu - 1)]} \tag{2-3}$$

where k_{eq} is the secant stiffness at maximum deformation.

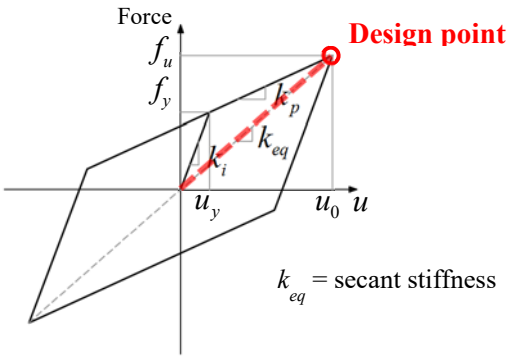

Figure 2.3 Secant stiffness concept

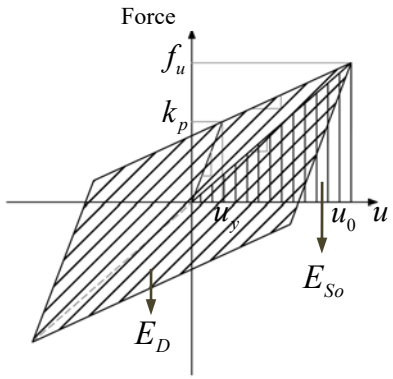

Figure 2.4 Equal energy dissipation principle

For the derivation of damping ratio, Rosenblueth and Herrera employed the equal energy dissipation principle which was first proposed by Jacopsen (Figure 2.4). According to this principle, defining equivalent viscous damping is to equate the energy dissipated in a vibration cycle of the actual structure and an equivalent viscous system. The total equivalent damping ratio can be expressed as

$$\xi_{eq} = \xi_0 + \xi_{hyst} \tag{2-4}$$

where ξ_0 is the viscous damping ratio that the structure has inherently, and ξ_{hyst} is the dissipated energy by hysteretic behavior of the isolation system. Under the condition $\omega = \omega_n$, where the response of the system is most sensitive to damping, damping ratio by hysteretic behavior ξ_{hyst} is expressed by

$$\xi_{hyst} = \frac{E_D}{4\pi E_{S0}} \tag{2-5}$$

$$E_D = \pi c \omega u_0^{\,2} = 2\pi\xi \frac{\omega}{\omega_n} k u_0^{\,2} \tag{2-1}$$

$$E_{S0} = \frac{1}{2} k u_0^{\,2} \tag{2-7}$$

where E_D is hysteretic energy dissipated per cycle of motion through inelastic deformation and E_{S0} means the elastic strain energy based upon secant stiffness.

Equation (2-4) can be rewritten as equation below in terms of the post-to-pre yield stiffness ratio α and the displacement ductility ratio μ

$$\xi_{eq} = \xi_0 + \xi_{hyst} = \xi_0 + \frac{2(1-\alpha)(\mu-1)}{\pi\mu[1+\alpha(\mu-1)]} \tag{2-8}$$

R&H method is also referred to as geometric stiffness method, which has been adopt by ASSHTO, Eurocode 8, and the new Italian code.

Dicleli and Buddaram

Dicleli and Buddaram found that the behavior of isolation system is affected by the peak ground acceleration to peak ground velocity ratio as well as the intensity of the ground motion relative to the characteristic strength of the isolator. It was also demonstrated that the equation of equivalent viscous damping ratio used in the design of base isolated structures must incorporate the equivalent period of the structure and the frequency characteristics of ground motion in order to acquire a more accurate estimation of seismic response quantities. From the regression analysis through various conditions shown in Figure 2.5, Dicleli and Buddaram proposed new equivalent damping ratio equation by modifying R&H method to include the period shift term. Modified equation is expressed as

$$\xi_{eq} = \xi_0 + \frac{2(1-\alpha)(\mu-1)}{\pi\mu[1+\alpha(\mu-1)]}\sqrt{0.41\left(\frac{T_{eq}}{T_0}-1\right)} \tag{2-9}$$

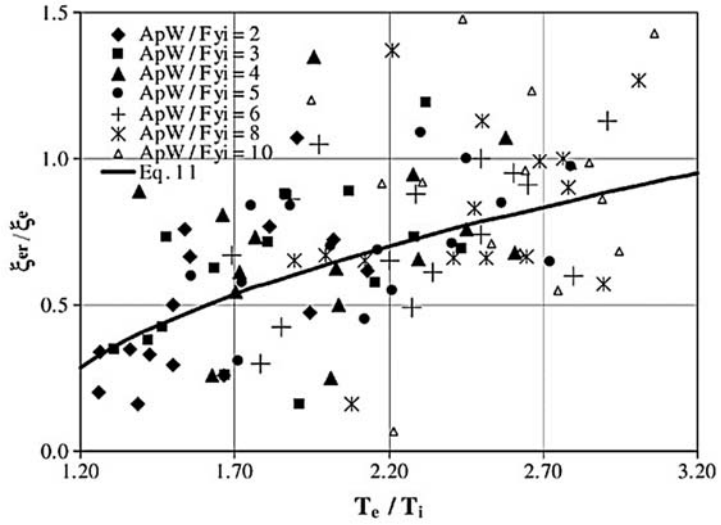

Figure 2.5 Ratio of actual effective damping to effective damping calculated using R&H method as a function of the effective period shift

where the term (T_{eq}/T_o – 1) means relative period shift that fulfills more accurate estimation.

Liu and Zordan

Liu and Zordan noted that EL properties of seismic isolation system are only related to the ductility ratio and pro-to-pre yield stiffness ratio in R&H method despite many specifications require additional conditions in order to substitute the nonlinear behavior for equivalent linear behavior. Figure 2.6 illustrates the feasible region of equivalent linearization of seismic isolation system. Liu and Zordan evaluated the suitability of limited conditions for equivalent linearization of seismic isolation system. Results revealed that, although adequate estimates can be obtained if the limited conditions are met, the application boundary of equivalent linearization of seismic isolation system

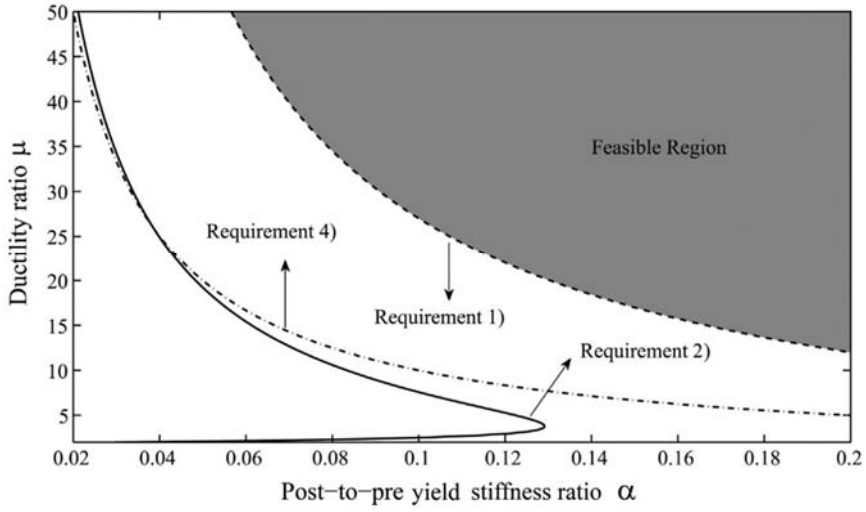

Figure 2.6 Feasible region of equivalent linearization of seismic isolation system

is significantly restricted. To improve the prediction accuracy of EL method in a wider parameter space, R&H method was modified through introducing a factor, which is related to ductility ratio μ, post-to-pre yield stiffness ratio α and initial period of seismic isolation system T_0. For base isolated structure with low ductility or large initial period, decreased damping ratio was applied. Modified EL method is expressed as

$$\xi_{eq} = \xi_0 + \frac{2(1-\alpha)(\mu-1)}{\pi\mu[1+\alpha(\mu-1)]} \Bigg/ \left((0.7763+0.2886T_0) + \frac{(0.5651+1.8410T_0}{\exp(\alpha\mu)} \right) \quad (2\text{-}10)$$

2.3.2 EL methods base upon empirical formulas

Secant stiffness based methods have several disadvantages. First, it is derived based on perfectly harmonic frequency condition, so this method is accurate for specific cases. But actual earthquake consists of wide-band

frequencies. Second, equivalent damping ratio is computed against maximum displacement u_0 despite there is only few moment isolator reaches to maximum displacement under earthquake. For this reason, error can occur by using EL methods base upon secant stiffness concept. So several researchers tried to derive EL methods base upon empirical formulas in order to decrease the error. In this study, methods proposed by Hwang and Chiou, and Guyader and Iwan is considered. Similar to the first group, they are abbreviated as H&C, and G&I.

Hwang and Chiou

Hwang and Chiou proposed an EL elastic method for the analysis of base isolated bridges with LRBs, which was derived in a modified form from AASHTO guide specifications for seismic isolation through an identification method or R&H method. They argue that EL methods proposed in the past are derived based on a possible maximum structural ductility ratio of 10 or less due to the fact that for most traditional earthquake-resistant structures a structural ductility ratio of 10 or less could be the maximum that the structures can sustain without severe damage or collapse. However, a LRB installed in a base isolated structure may experience very large deformations during a major quake. As indicated in the Table 2.1, H&C method include a total of 15 ductility ratios up to 50.

The results are fitted to the AASHTO curve. Figure 2.7 shows the results of the analysis. It can be found that period shifts and equivalent damping ratios are more scattered corresponding to small ductility ratios than large ductility ratios. The provided formulas for computing period ratio and equivalent viscous damping ratio by regression analysis are respectively expressed as

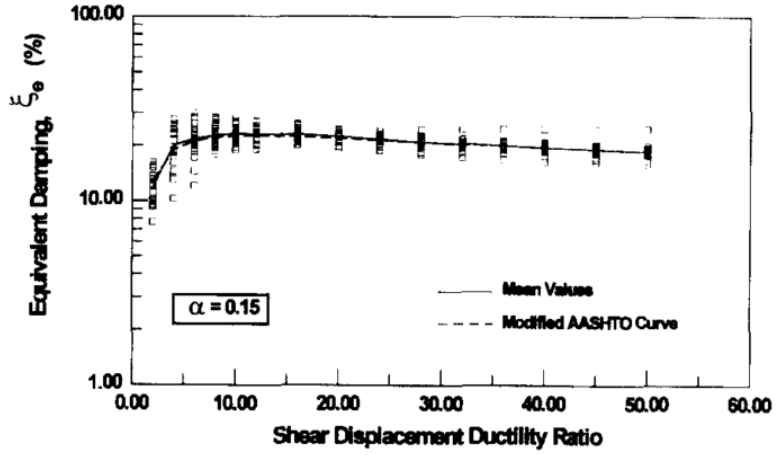

(a)

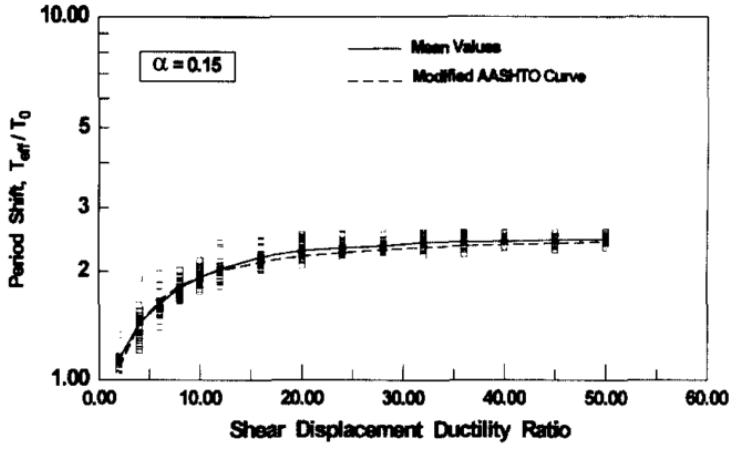

(b)

Figure 2.7 (a) Summary of identified effective period shift; (b) summary of identified equivalent damping ratios. Both compare mean values with fitted curve

$$T_{eq}/T_0 = \sqrt{\frac{\mu}{1+\alpha(\mu-1)}}\left(1-0.737\frac{\mu-1}{\mu^2}\right) \tag{2-11}$$

$$\xi_{eq} = \xi_0 + \frac{2(1-\alpha)(\mu-1)}{\pi\mu[1+\alpha(\mu-1)]}\frac{\mu^{0.58}}{6-10\alpha} \tag{2-12}$$

Guyder and Iwan

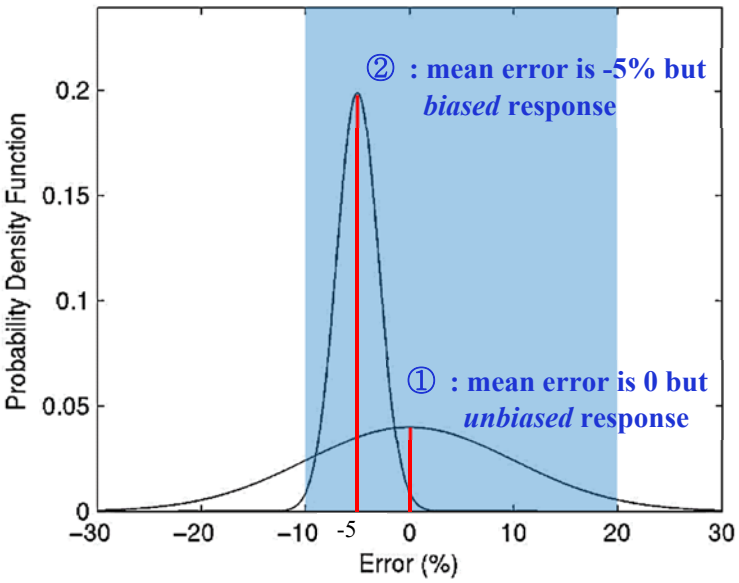

Figure 2.8 Illustration of probability density function for a normal distribution

In order to achieve more accurate response of structure by optimal EL parameters according to some sense of engineering acceptability, Guyader and Iwan introduced the standard deviation as the index of the accuracy estimation. In Figure 2.8, there are two types of normal distribution curves. By other EL methods, curve ① would be more accurate result because it's mean error is zero, but it's results is unbiased, or scatteredness of result is big. On the other hand, curve ② has 5 % error in mean value but more biased, or scatteredness of curve ② has 5 % error in mean value but it is more biased, or scatteredness of result is small. In G&I method, the optimal pair of T_{eq} and ξ_{eq} were taken as the values that minimize the probability that the percentage error between the actual nonlinear systems lies outside some desired range -10 % to +20 %. They expressed that concept through

$$\boldsymbol{R_{EAR}} \equiv 1 - \Pr(-10\% < \boldsymbol{\varepsilon_D} < 20\%) = \boldsymbol{minimum} \tag{2-13}$$

where R means the probability that the error, ε_D, lies outside some desired range.

To cover nonlinear hysteresis similarly, this method considered several behaviors including bilinear, stiffness degrading, strength degrading and pinching hysteresis methods as indicated in Table 2.1. By curve fitting process, analytical expressions were proposed for three range sorted by ductility ratio. This method had been adopted as one of the three solution procedures to be presented in FEMA-440.

For $\mu < 4.0$:

$$T_{eq} / T_0 = 1 + 0.1262(\mu - 1)^2 - 0.0224(\mu - 1)^3 \tag{2-14}$$

$$\xi_{eq} = \xi_0 + 0.05073(\mu - 1)^2 - 0.01083(\mu - 1)^3 \tag{2-15}$$

For $4.0 \le \mu \le 6.5$:

$$T_{eq} / T_0 = 1.1713 + 0.1194(\mu - 1) \tag{2-12}$$

$$\xi_{eq} = \xi_0 + 0.1169 + 0.01579(\mu - 1) \tag{2-17}$$

For $\mu > 6.5$:

$$T_{eq} / T_0 = 1 + 0.87\left(\sqrt{\frac{\mu - 1}{1 - 0.10\left[(\mu - 1) - 1\right]}} - 1\right) \tag{2-18}$$

$$\xi_{eq} = \xi_0 + 0.1169 + 0.01579(\mu - 1) \tag{2-19}$$

Chapter 3. Critical Evaluation of EL Methods

3.1 General

In this chapter, the response aspects of model characterized by multi-degree-of-freedom system is analyzed. The 20 sets of earthquake data scaled to DBE and MCE level of California design spectrum are applied to 5 story model (6 DOFs). This chapter contains two types of analysis results. Peak displacement response at the base floor and peak acceleration response at roof floor are derived by using equivalent linear method and nonlinear method respectively. From the result, response accuracy of each EL methods are evaluated.

The result is arranged by the mean and standard deviation of relative displacement of base floor and peak absolute acceleration of roof floor.

3.1.1 Analysis model

5 story shear building from Kelly's research (Kelly, 1987) is considered as the analysis model. This model is experimental model. Story height is 3 m and properties of mass and lateral stiffness are derived from full scale test specimen. Damping coefficient values are adjusted to satisfy 2% damping at 1^{st} and 2^{nd} mode of superstructure by using Rayleigh damping method. 1^{st} mode period of superstructure is 0.31 sec and 2^{nd} mode period is 0.11 sec.

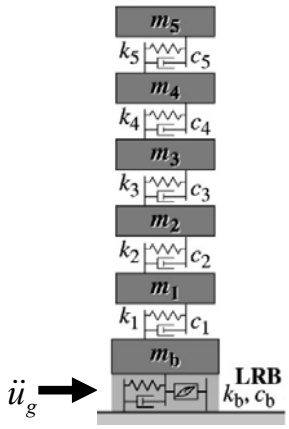

Figure 3.1 Analysis model

Table 3.1 Model properties

Floor masses (kg)	Lateral stiffness (kN/m)	Damping coefficients (kN·s/m)
m_b = 6800	k_b = 0	c_b = 0
m_1 = 5897	k_1 = 33732	c_1 = 67
m_2 = 5897	k_2 = 29093	c_2 = 58
m_3 = 5897	k_3 = 28621	c_3 = 57
m_4 = 5897	k_4 = 24954	c_4 = 50
m_5 = 5897	k_5 = 19059	c_5 = 38

3.1.2 Earthquake ground motions

Forty ground motions from FEMA (somerville, et al, 1997) are included in this study. The target response spectra for this study are for NEHRP site category S_D, firm soil. Preference was given to time histories recorded on site category S_D, but recordings from rock conditions and simulated recordings were also included. These rock site recordings and simulated recordings were modified for site conditions. Considered earthquake recordings cover various types of epicentral distance, duration, strong motion duration. Also with including broad-band and narrow-band frequencies, the data have generality.

The FEMA report states the detail of the scaling procedure,

> *A single scaling factor was found which minimized the squared error between the target spectrum and the average response spectrum of the two horizontal components of the time history assuming lognormal distribution of amplitudes. The scale factor that minimized the weighted sum of the squared error between the target values and the average of the two*

> *horizontal components was calculated. The weights used were 0.1, 0.3, 0.3, and 0.3 for periods of 0.3, 1, 2, and 4 seconds respectively. The scale factor was then applied to all three components of the time history. This procedure retained the ratios between the three components at all periods.*

Table 3.2 indicates suite of ground motions for a 10% in 50 years seismic hazard (LA01-LA20), representing the DBE ground motions, and Table 3.3 indicates suites of ground motions for a 2% in 50 years seismic hazard (LA21-LA40), representing the MCE ground motions. Mean PGA of each earthquake group is 0.59g and 0.88g respectively.

Figure 3.2 and Figure 3.3 show the response spectrum plots with 5% damping ratio for these ground accelerations. Bold line indicates the mean of the peak pseudo accelerations for each earthquake records. From Figure 3.2, large pseudo acceleration occurs when the natural period of the structure is short as zero to 1.5 sec with DBE level earthquakes. To make enough period shift for mitigate the damage, natural period seems to be over 2 sec where pseudo acceleration is under 0.5g. For MCE level earthquakes, period seems to be over 2.5 sec to achieve enough period shift.

Table 3.2 Considered earthquake ground motions (DBE level)

EQ code	Description	Magnitude	Distance (km)	Scale Factor	Time Step (sec)	PGA (g's)
la01	1940 Imperial Valley	6.9	10.0	2.01	0.020	0.46
la02	1940 Imperial Valley	6.9	10.0	2.01	0.020	0.68
la03	1979 Imperial Valley	6.5	4.1	1.01	0.010	0.39
la04	1979 Imperial Valley	6.5	4.1	1.01	0.010	0.49
la05	1979 Imperial Valley	6.5	1.2	0.84	0.010	0.30
la06	1979 Imperial Valley	6.5	1.2	0.84	0.010	0.23
la07	1992 Landers	7.3	36.0	3.20	0.020	0.42
la08	1992 Landers	7.3	36.0	3.20	0.020	0.43
la09	1992 Landers	7.3	25.0	2.17	0.020	0.52
la10	1992 Landers	7.3	25.0	2.17	0.020	0.36
la11	1989 Loma Prieta	7.0	12.0	1.79	0.020	0.67
la12	1989 Loma Prieta	7.0	12.0	1.79	0.020	0.97
la13	1994 Northridge	6.7	6.7	1.03	0.020	0.68
la14	1994 Northridge	6.7	6.7	1.03	0.020	0.66
la15	1994 Northridge	6.7	7.5	0.79	0.005	0.53
la16	1994 Northridge	6.7	7.5	0.79	0.005	0.58
la17	1994 Northridge	6.7	6.4	0.99	0.020	0.57
la18	1994 Northridge	6.7	6.4	0.99	0.020	0.82
la19	1986 North Palm Springs	6.0	6.7	2.97	0.020	1.02
la20	1986 North Palm Springs	6.0	6.7	2.97	0.020	0.99

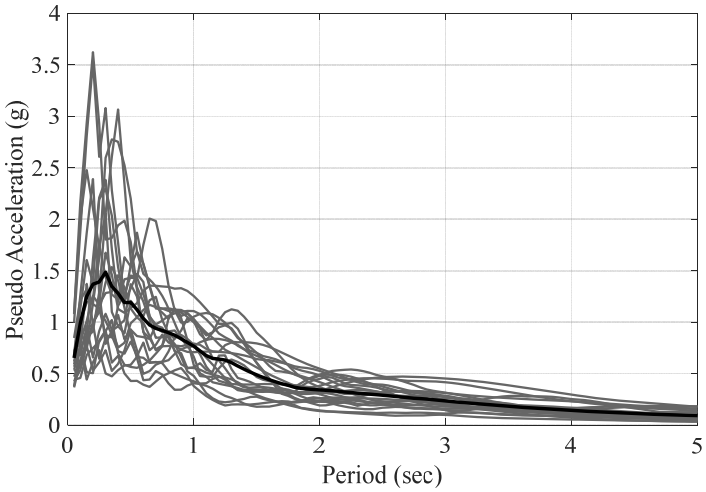

Figure 3.2 Response spectrum of 20 DBE earthquake data with 5% damping

Table 3.3 Considered earthquake ground motions (MCE level)

EQ code	Description	Magnitude	Distance (km)	Scale Factor	Time Step (sec)	PGA (g's)
la21	1995 Kobe	6.9	3.4	1.15	0.020	1.28
la22	1995 Kobe	6.9	3.4	1.15	0.020	0.92
la23	1989 Loma Prieta	7.0	3.5	0.82	0.010	0.42
la24	1989 Loma Prieta	7.0	3.5	0.82	0.010	0.47
la25	1994 Northridge	6.7	7.5	1.29	0.005	0.87
la26	1994 Northridge	6.7	7.5	1.29	0.005	0.94
la27	1994 Northridge	6.7	6.4	1.61	0.020	0.93
la28	1994 Northridge	6.7	6.4	1.61	0.020	1.33
la29	1974 Tabas	7.4	1.2	1.08	0.020	0.81
la30	1974 Tabas	7.4	1.2	1.08	0.020	0.99
la31	Elysian Park (simulated)	7.1	17.5	1.43	0.010	1.30
la32	Elysian Park (simulated)	7.1	17.5	1.43	0.010	1.19
la33	Elysian Park (simulated)	7.1	10.7	0.97	0.010	0.78
la34	Elysian Park (simulated)	7.1	10.7	0.97	0.010	0.68
la35	Elysian Park (simulated)	7.1	11.2	1.10	0.010	0.99
la36	Elysian Park (simulated)	7.1	11.2	1.10	0.010	1.10
la37	Palos Verdes (simulated)	7.1	1.5	0.90	0.020	0.71
la38	Palos Verdes (simulated)	7.1	1.5	0.90	0.020	0.78
la39	Palos Verdes (simulated)	7.1	1.5	0.88	0.020	0.50
la40	Palos Verdes (simulated)	7.1	1.5	0.88	0.020	0.63

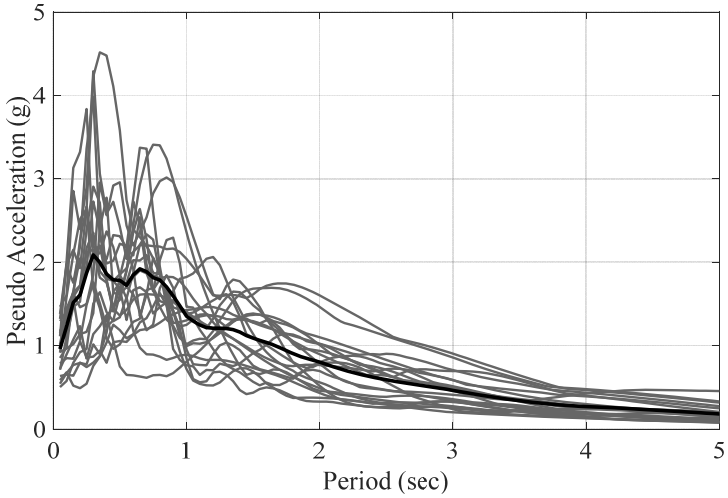

Figure 3.3 Response spectrum of 20 MCE earthquake data with 5% damping

3.1.3 Parameters included in this study

Fixed parameters

Before examine the responses of structure, basic properties of LRB were determined. Main properties of isolator are post-to-yield ratio α and normalized yield strength Q_y.

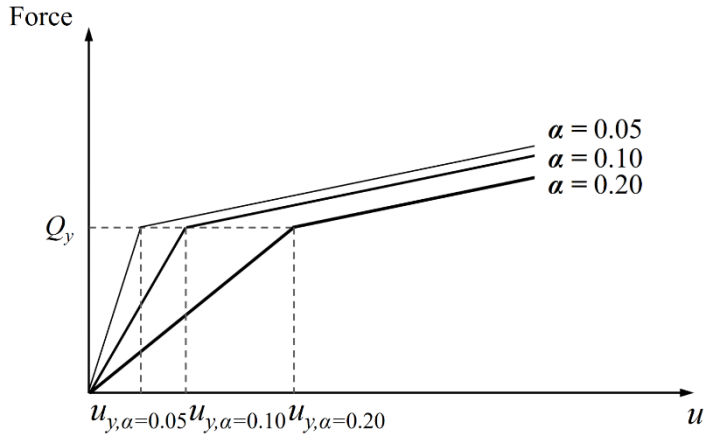

Figure 3.4 Aspects of hysteresis with α change

Figure 3.4 shows the aspect of hysteretic behavior of isolator with α change. It is in charge of the yield displacement of the isolator in that when isolated period T_p is given, isolator yields at larger displacement as α increases. Meanwhile yield strength normalized with total weight of superstructure Q_y (= f_y/W) is another important property of isolator. It means the force that triggers the isolator to operate flexibly.

Figure 3.5 (a) and (b) indicate the response of base deformation and roof acceleration with various Q_y value respectively. It can be shown that as Q_y increases, base deformation decreases but acceleration of roof floor increases significantly. Also, as α increases, base deformation increases but roof acceleration increases. By considering two different aspects, 5% for Q_y value and 0.1 for α is applied for LRBs in this study.

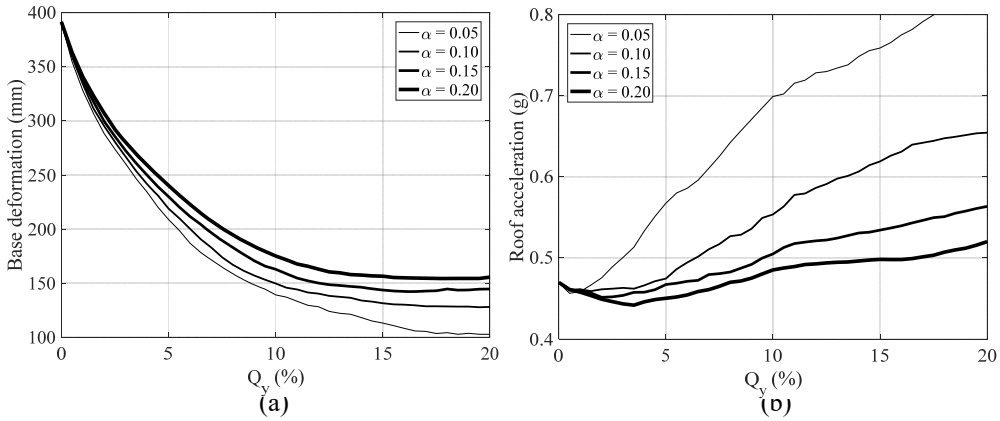

Figure 3.5 (a) Response of base deformation with Q_y changes (b) response of roof acceleration with Q_y change

Variables

To examine the responses of structure with different design conditions, two variables are considered in this study. One variable is fundamental period of isolated structure T_p. By assuming enough period shift is achieved, T_p varies from 1.5 sec to 3.0 sec with increment equal to 0.5 sec where acceleration effect is not critical in response spectrum of DBE and MCE earthquake input (Figure 3.2, Figure 3.3). The other variable is design maximum displacement u_0. To include wide range of isolator deformation, from 0.1m to 0.4m with increment equal to 0.1m were considered as u_0. Figure 3.6 (a) and (b) describe the aspect of transition as each variable changes. It can be noticed that ductility ratio increases as isolated period T_p shortened and design maximum displacement u_0 increases. Ductility ratio means the deformation capacity of isolator after yielding.

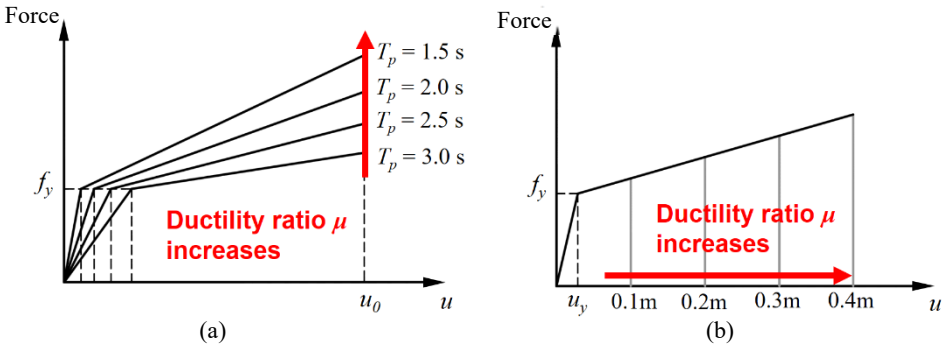

Figure 3.6 (a) Aspect of transition with Tp change; (b) aspect of transition with u_0 change

Table 3.4 indicates the ductility ratio considered in this study, which is range from 9.0 to 143.2. Some of ductility ratio values are somewhat big but also considered to examine the response aspects.

Table 3.4 Ductility ratios considered in this study

Max. displacement u_0 (m)	Isolated period T_p (sec)	μ
0.1	1.5	35.9
	2.0	19.3
	2.5	13.0
	3.0	9.0
0.2	1.5	71.8
	2.0	40.3
	2.5	25.8
	3.0	17.9
0.3	1.5	107.4
	2.0	60.7
	2.5	38.6
	3.0	26.9
0.4	1.5	143.2
	2.0	80.6
	2.5	51.6
	3.0	35.8

3.1.4 Evaluation procedure

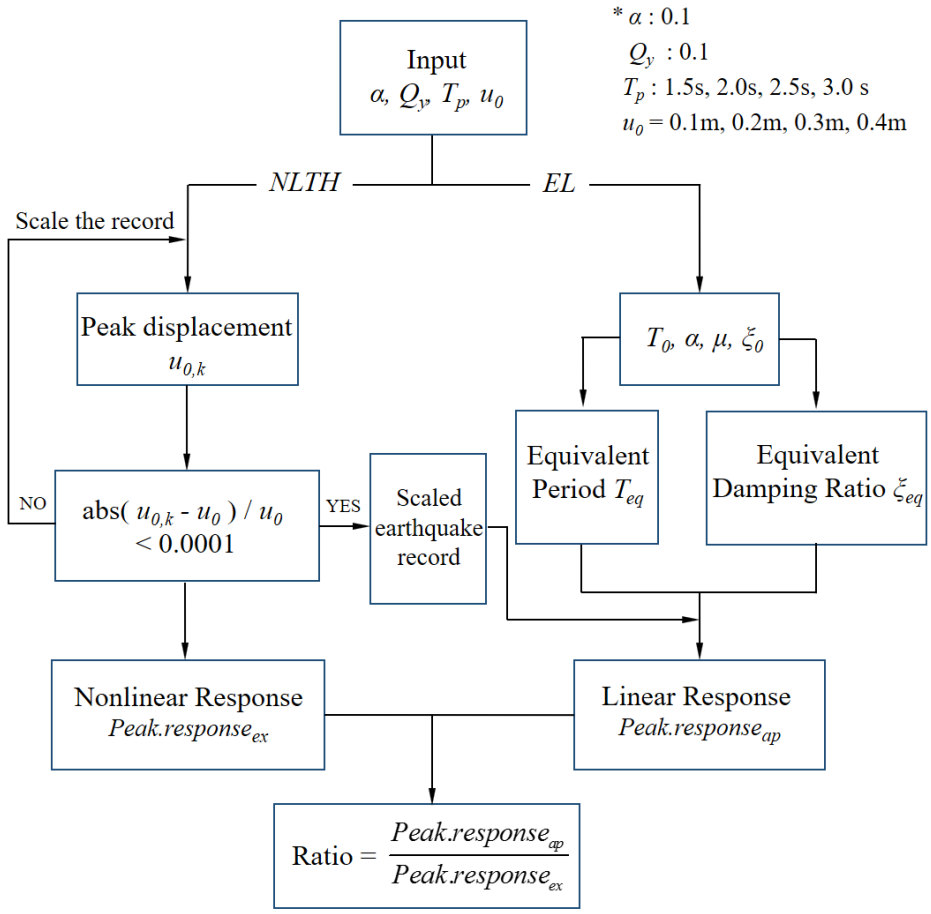

Figure 3.7 Flowchart of the process

The accuracy of different EL methods is examined through comparison of results between nonlinear time history (NLTH) analysis and EL method. As illustrated in Figure 3.7, an iterative scaling process of the selected ground motion was performed until the computed peak displacement $u_{0,k}$ is enrolled in error range of 0.0001, compared to the desired maximum displacement u_0. NLTH analysis was conducted using complicated Runge-Kutta numerical method by MATLAB program. After the scale factors are determined, scaled

earthquake records are applied to EL method with predefined ductility ratios and hysteretic characteristics of the systems.

3.2 Responses of Equivalent Linear Analysis and Nonlinear Analysis

As the earthquake data listed in Table 3.2 and Table 3.3 is re-scaled by the process indicated in Figure 3.7. So these data cannot be categorized by DBE or MCE level earthquake. In this section, results of structure are categorized by set *A* and set *B* which are modified form of DBE and MCE level earthquake sets respectively.

3.2.1 Analysis indicators

As the indicators to evaluate EL methods, relative displacement and absolute acceleration of superstructure were selected. Relative displacement indicates the damage of structure that severe interstory drift can occur collapse of structure. As indicated in preceding chapter, most of the deformation is concentrated at base floor because of the low lateral stiffness. So, relative displacement of base floor was chosen as analysis indicator when evaluate the accuracy of EL methods in this study. On the other hand, absolute acceleration is another important indicator that non-structural members and equipment inside of the building are more affected by their own inertial force than relative acceleration. Absolute acceleration determines the substantive performance of the structure so it is particularly critical to the buildings which have high

importance factor such as data center, hospital, or nuclear power facilities.

The indicators arranged by the mean ratio of maximum responses and standard deviation of maximum responses. Mean ratio R of maximum responses is expressed as

$$R = \frac{1}{N}\sum_{l=1}^{N}\frac{Peak.response_{\mathrm{ap},l}(T_{eq},\xi_{eq})}{Peak.response_{\mathrm{ex},l}(T_0,\alpha,\mu,\xi_0)} \tag{3-1}$$

where N means the number of earthquake data. If R is higher than 1, equivalent method overestimates the responses as compared with nonlinear method. On the opposite, if R is lower than 1, equivalent method underestimates the responses as compared to responses of nonlinear method. Meanwhile, standard deviation can be expressed as

$$\sigma(R) = \sqrt{\frac{1}{N-1}\sum_{l=1}^{N}\left(\frac{Peak.response_{\mathrm{ap},l}(T_{eq},\xi_{eq})}{Peak.response_{\mathrm{ex},l}(T_0,\alpha,\mu,\xi_0)} - R\right)^2} \tag{3-2}$$

where N means the number of earthquake data. Standard deviation means the scatteredness of responses for each input data, namely the reliability of the EL methods.

3.2.2 Relative displacement of roof floor

Set A earthquake response

Figure 3.8 and Figure 3.9 illustrates the mean ratio R and standard deviation σ evaluation results of relative displacement at base floor under set A earthquakes respectively. Note that, in order to compare more clearly, boundary of the plot range in vertical axes of all different EL methods are fitted identically.

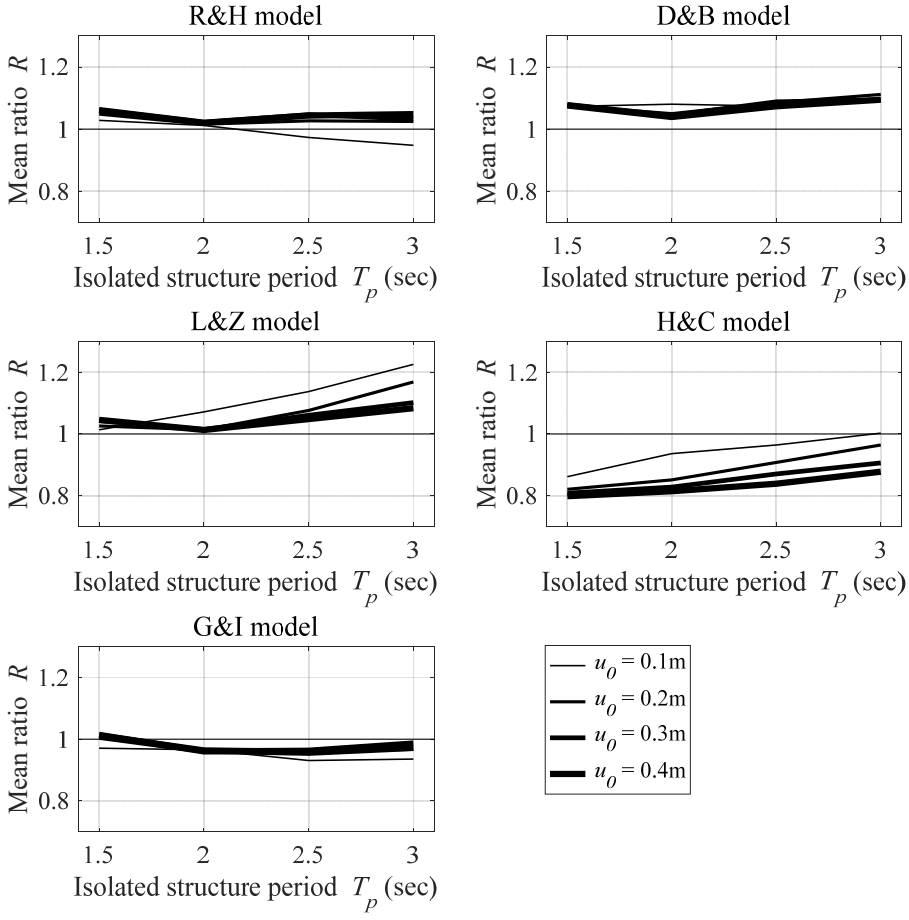

Figure 3.8 Estimation accuracy mean ratio *R* of relative displacement at base floor based on each EL methods under set *A* earthquakes

Remind that, as referred in subsection 3.1.3, ductility ratio μ increases as isolated period T_p shortened and design maximum displacement u_0 increases.

R&H method shows generally accurate estimation of relative displacement as mean ratio *R* with the error less than 10 percent. R&H method slightly overestimate the response of structure in the majority cases, but when

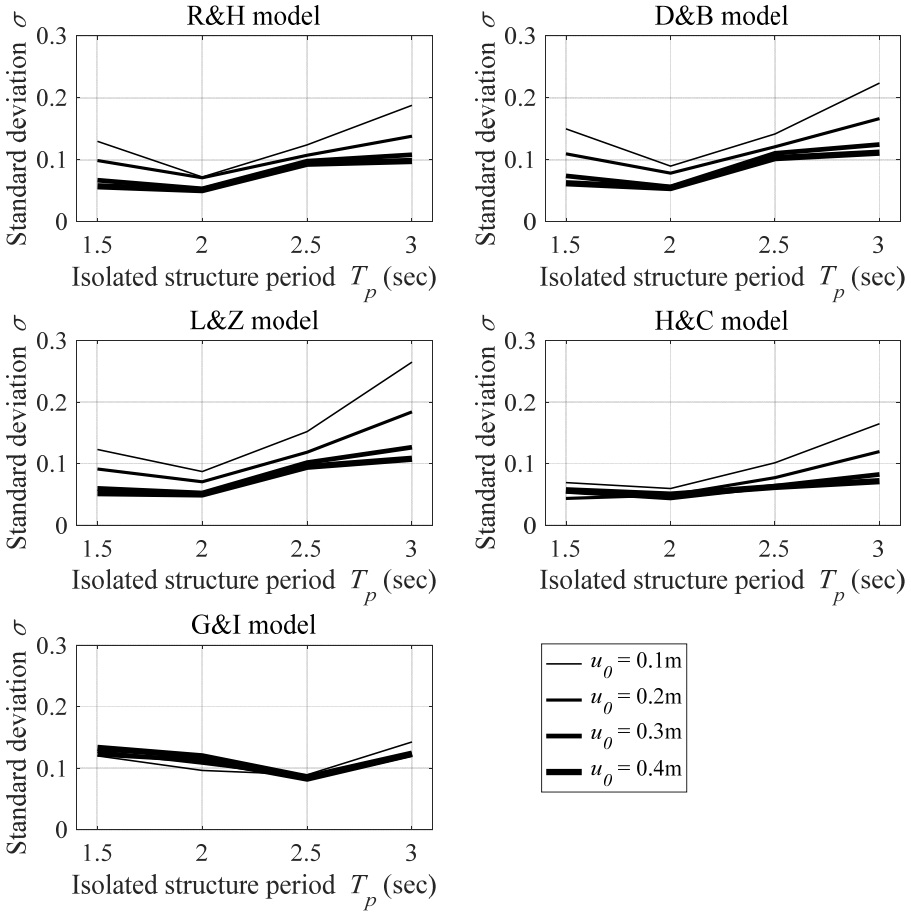

Figure 3.9 Standard deviation of mean ratio *R* of relative displacement at base floor based on each EL methods under set *A* earthquakes

u_0 equals to 0.1m, response was underestimated. Effect of the variables such as design maximum displacement and isolated structure period is not well defined. When it comes to standard deviation, as ductility increases, responses turn out to be more biased in general. Especially, standard deviation is relatively large when design displacement is 0.1 m.

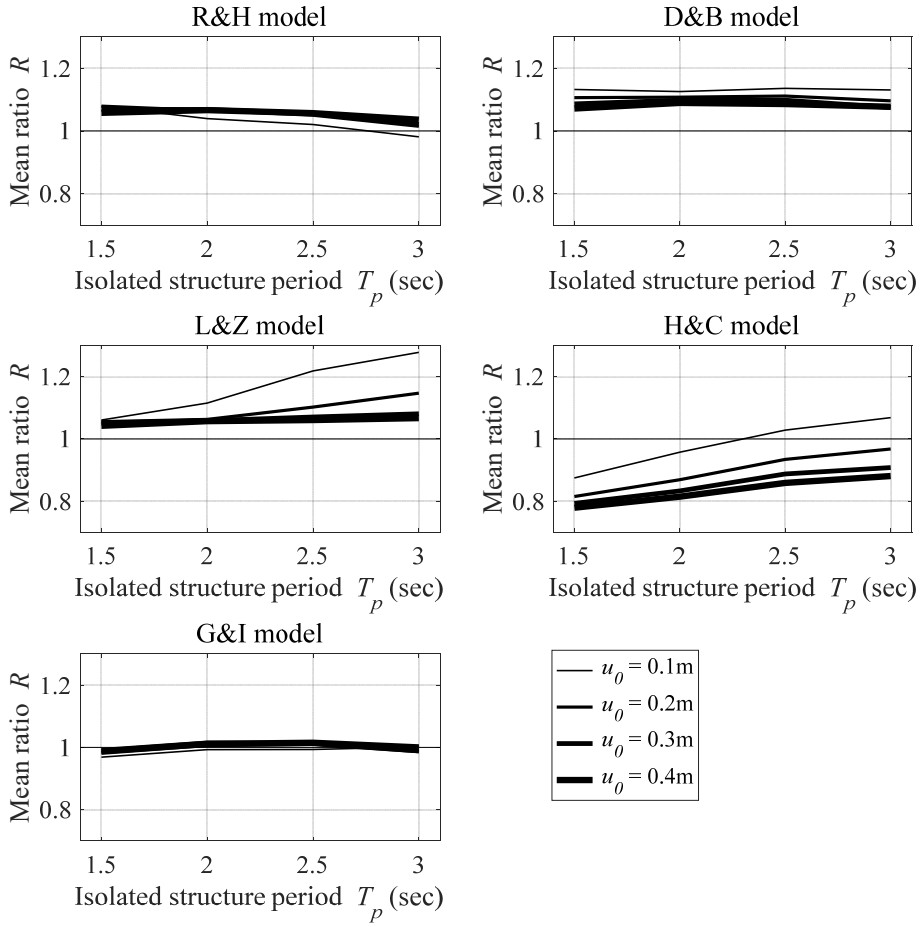

Figure 3.10 Estimation accuracy mean ratio *R* of relative displacement at base floor based on each EL methods under set *B* earthquakes

Results aspect of D&B method is similar with R&H method in both mean ratio and standard deviation. D&B method estimated the response slightly larger (overestimated) and effect of both variables that include design maximum displacement and isolated structure period is not that remarkable. On the sight of standard deviation, responses values are slightly more scattered than R&H. L&Z method also showed similar results with R&H and D&B

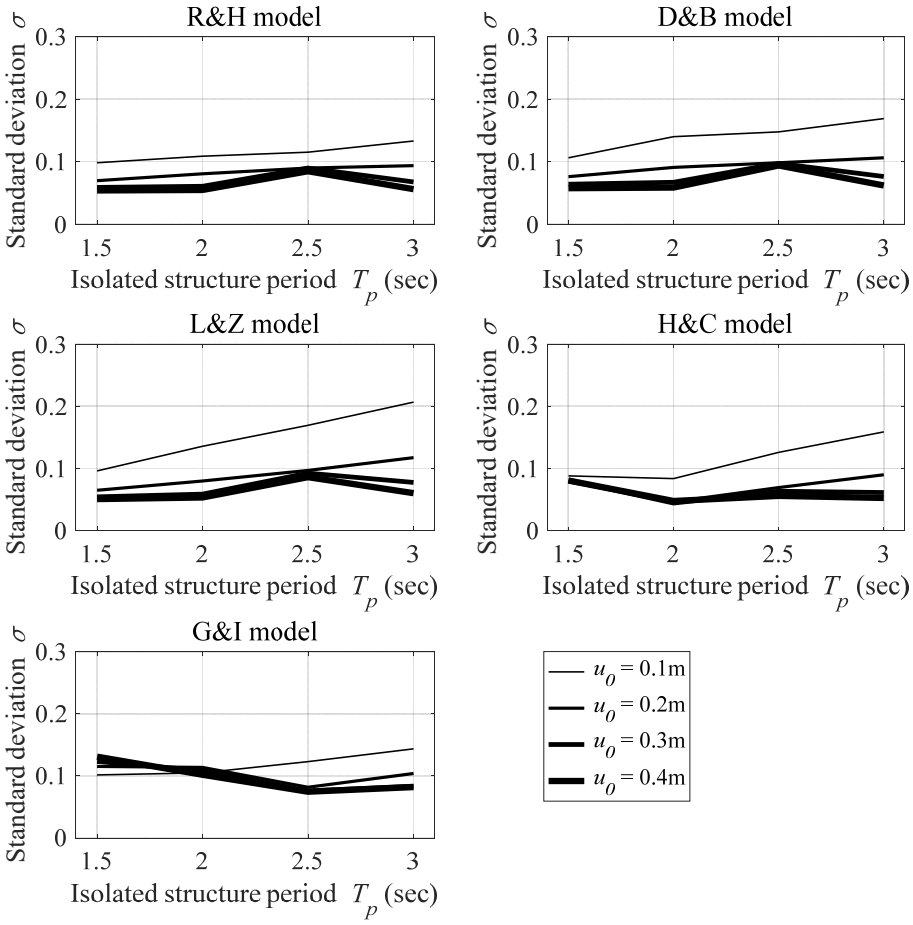

Figure 3.11 Standard deviation of mean ratio *R* of relative displacement at base floor based on each EL methods under set *B* earthquakes

methods for high ductility cases. However, for low ductility cases, the responses of relative displacement were significantly overestimated and standard deviations were also large (isolated structure period is relative long and design maximum displacement is 0.1m or 0.2m). The maximum error is up to 22 percent for systems with isolated period of 3.0 sec and design displacement of 0.1 m. Despite the three above-mentioned methods, H&C underestimates the

response. Especially, as ductility ratio increases, estimation accuracy of the mean ratio decreases. The maximum error is up to 21 percent. If the structure is designed with underestimated responses, deformation that exceed the design displacement can occurs under actual earthquake excitations. In that case, isolation system cannot operate properly, so H&C method needs to be improved for more accurate estimation. When EL method proposed by Guyader and Iwan used, responses are slightly underestimated but scatteredness of response with design displacement change is significantly lower than any other methods. Standard deviation of G&I method is also biased compared to other EL methods regardless of variables with design maximum displacement. The standard deviation is in the order of 0.1. It is because this method considered not only the mean value but also the standard deviation of peak responses.

Set B earthquake response

From R&H method, the accuracy estimation of relative displacement mean ratio under set *B* earthquakes, results aspect is similar with aspect under set *A* earthquakes. Maximum displacement is generally slightly overestimated for most conditions except for the case that design displacement is 0.1 m and isolated period is 3.0 sec (ductility ratio is small), but overall this method shows quite accurate estimation with error less than 10 percent. Standard deviation is mitigated compared to set *A* cases.

D&B method overestimates the mean ratio of peak relative deformation. It seems that as design maximum displacement increases, estimation accuracy increases and results are not affected by the isolated period of the structure. Standard deviation decreases as ductility ratio increases. Despite standard deviation is on the order of 0.1 in most cases, standard deviation is relatively

large when design displacement is 0.1 m.

L&Z method tends to yield conservative estimates of the maximum inelastic displacement. The estimation accuracy increases as isolated period shortened for the cases design maximum displacement 0.1 m and 0.2 m but the effect is not applied to the larger cases. Maximum error occurs up to 28 percent when u0 is 0.1 m and isolated period is 3.0 sec. Standard deviation is also large when u0 is 0.1 m, but scatteredness is in the order of 0.1 for other cases.

H&C method generally underestimates the peak response of structure significantly except few cases. As the design maximum displacement increases and isolated period is shortened, the estimation of the peak response decreases. The maximum error occurs up to 22 percent. Despite of the underestimation of the peak response value, standard deviations of each conditions remains within 0.1 except for the case u_0 is 0.1 m.

Good estimations are obtained corresponding to G&I method and relative errors are on average smaller than 5 percent. In general, regarding standard deviation of the measured ratios, larger dispersions will be obtained for relatively low ductility ratios, and the isolated period has no significant effect in the standard deviation.

3.2.3 Absolute acceleration of base floor

Set A earthquake response

This subsection includes the absolute acceleration response of roof floor. Figure 3.12 and Figure 3.13 indicates the mean ratio and standard deviation results under set *A* earthquake excitations. Overall, it can be noted that all EL methods underestimate the responses except few cases of G&I method.

Mean ratio results corresponding to R&H method are almost similar with the results from D&B method and L&Z method. The maximum inelastic displacements are underestimated for all level of ductility ratio. There is no general trend of mean ratio with the change of design maximum displacement or isolated period. But when u_0 is 0.1 m, error occurs significantly, especially over 50 percent when isolated period is 2.0 sec. Although the peak inelastic displacements are underestimated, standard deviation of the measured ratio is within 0.2. Standard deviation results of R&H method decrease as ductility ratio increases in general.

D&B method and L&Z method shows slightly larger or lower results than R&H method respectively. As those three methods are based upon the secant stiffness concept, the acceleration is supposed to be affected mainly by equivalent lateral stiffness. 0.1 m can be somewhat small deformation capacity for base isolator but it is meaningful when it comes to performance based design for the structures having high importance factor such as hospitals or data centers as they are sensitive to the superstructure acceleration.

H&C method presents the mean approximate to exact displacement ratios is significantly underestimated over all range of variables. There is aspect that as isolated period is shortened, accuracy of estimation is decreases. As other EL

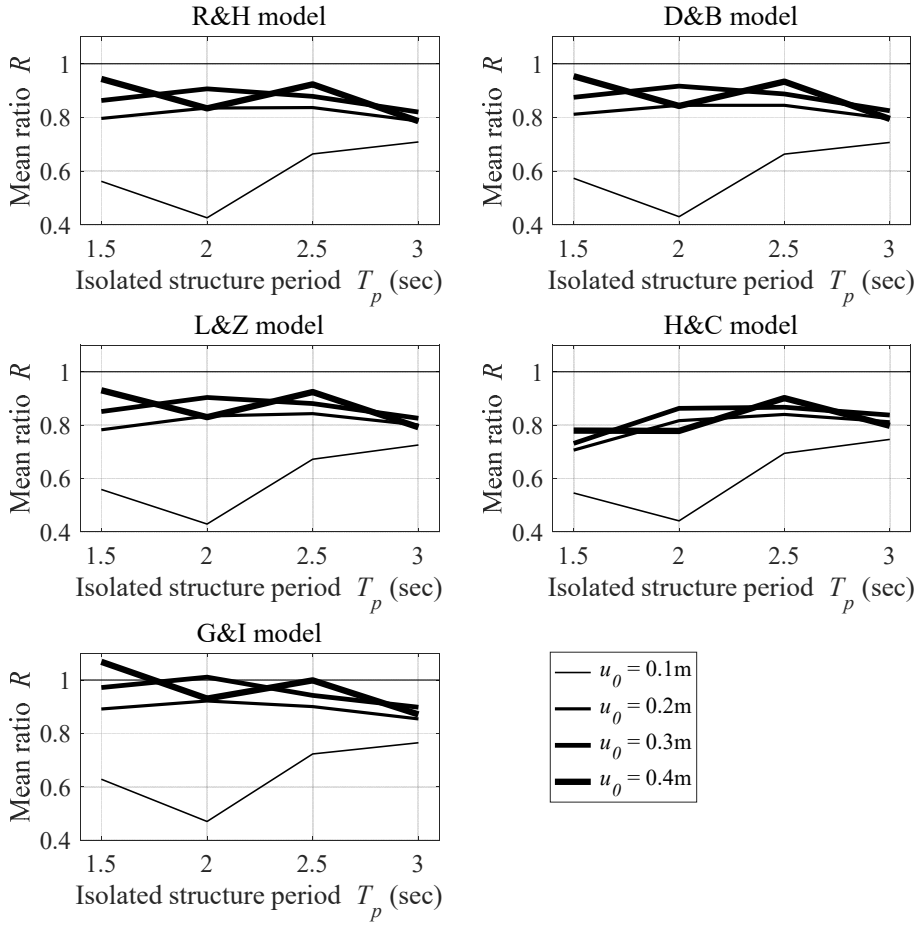

Figure 3.12 Estimation accuracy mean ratio *R* of absolute acceleration at roof floor based on each EL methods under DBE level earthquakes

methods, the results for the case where design maximum displacement is 0.1 m is especially underestimates the absolute acceleration of the roof floor. In the case case of standard deviation, H&C indicates that as the isolated period shortened, standard deviation decreases. Maximum standard deviation is 0.25.

Meanwhile, G&I method provides the most affordable response estimation of structure when design maximum displacement and ductility ratio

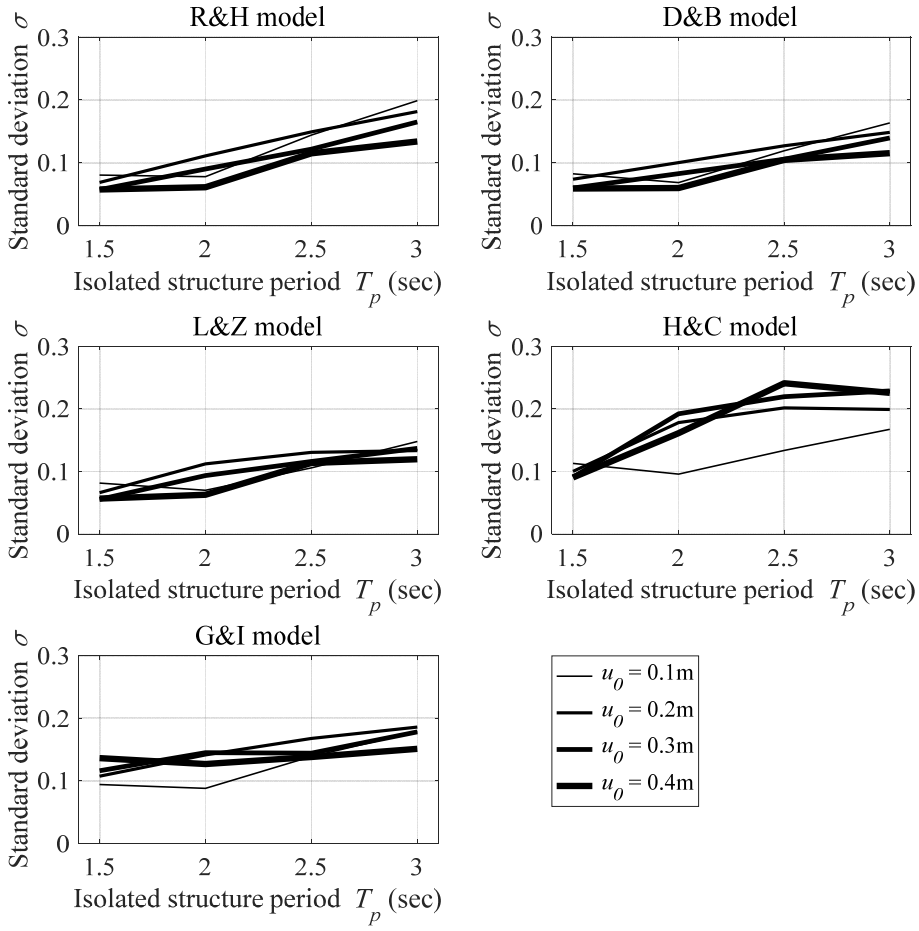

Figure 3.13 Standard deviation of mean ratio *R* of absolute acceleration at roof floor based on each EL methods under DBE level earthquakes

are relatively large. G&I method is considered to be more accurate than that from any other EL methods in that conditions. However, for the case that u_0 is 0.1, this method also underestimated the response of the structure significantly. In the standard deviation, the influence of design maximum displacement is not remarkable and as the isolated period shortend, standard deviation decreases.

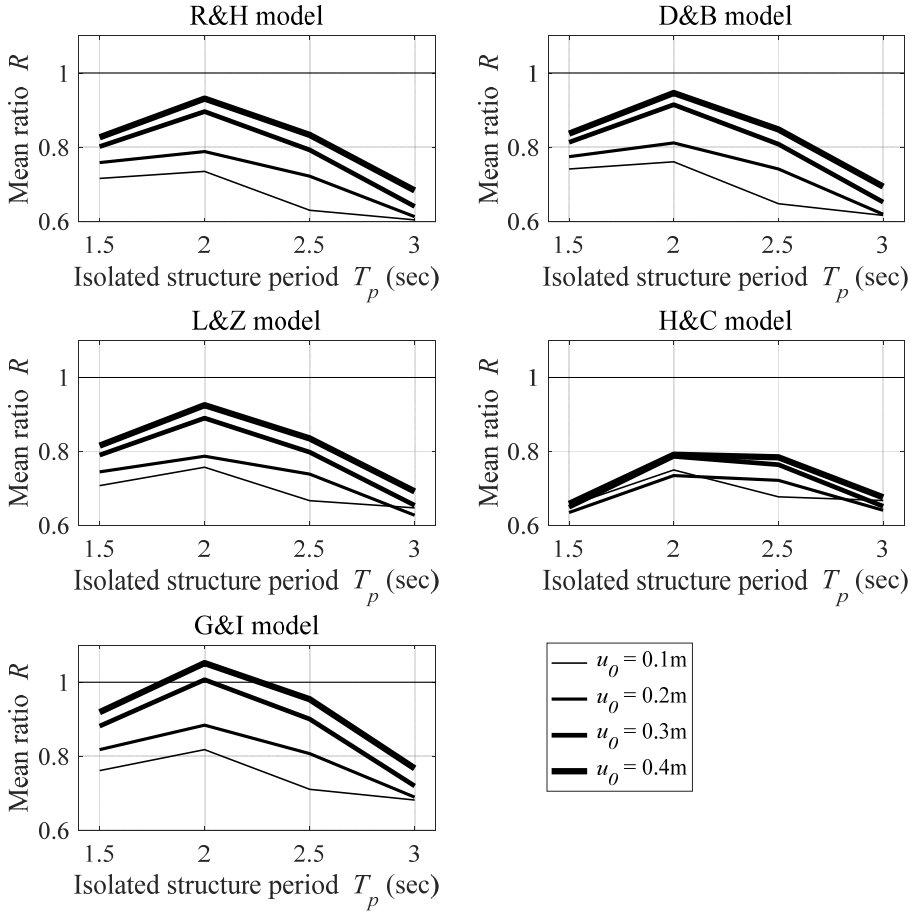

Figure 3.14 Estimation accuracy mean ratio *R* of absolute acceleration at roof floor based on each EL methods under MCE level earthquakes

Set B earthquake response

Mean ratio and standard deviation results of absolute acceleration responses at roof floor under set *B* earthquake excitation are illustrated in Figure 3.14 and Figure 3.15. Mean ratio results indicate that the EL method underestimates the response of structure in all cases, especially when the ductility ratio is small.

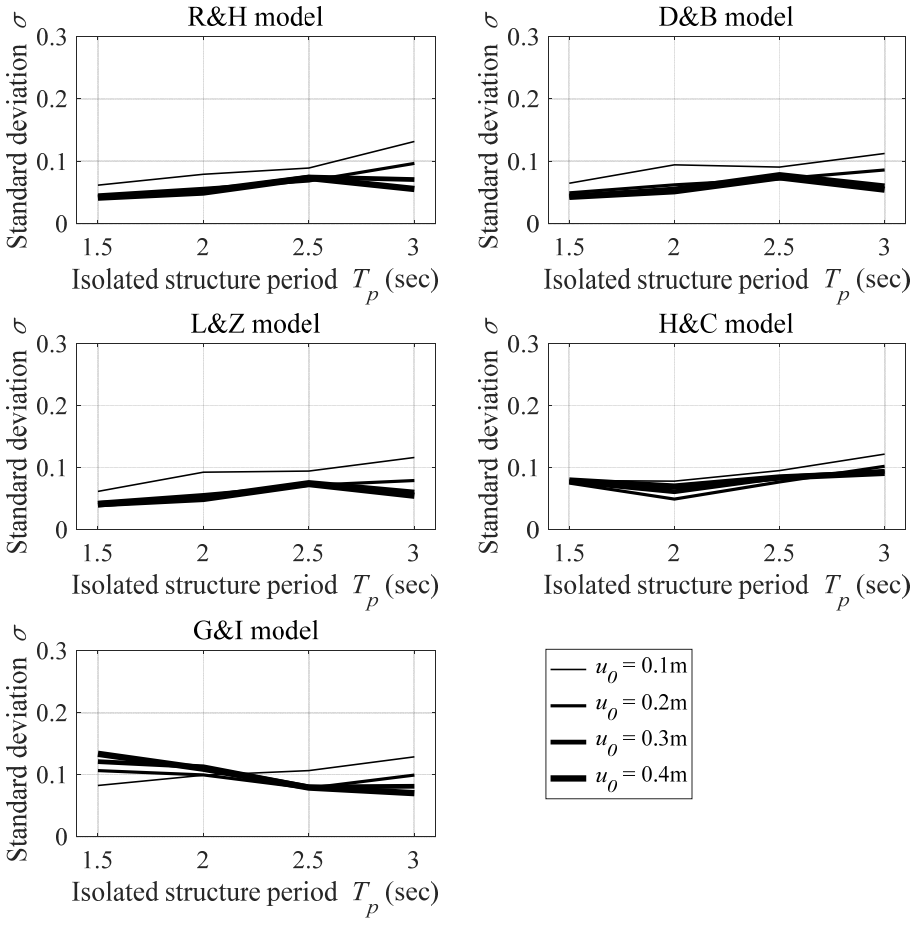

Figure 3.15 Standard deviation of mean ratio *R* of absolute acceleration at roof floor based on each EL methods under MCE level earthquakes

As the result under set *A* earthquakes, R&H, D&B, L&Z methods expect the similar responses. However, the aspect of response is different in that the variable change affects the response of the structure. It can be seen that estimation accuracy of absolute acceleration response increases as the design maximum displacement increases. In the respect of isolated period variable, estimation accuracy is highest when isolated period is 2.0 sec but still low

prediction was derived. Particularly, when the design displacement is 0.1 m, EL method seriously underestimates the response with the error up to 40 percent.

H&C method shows even more underestimated results than other methods. As the design maximum displacement increases, the accuracy increases slightly and there is no notable influence of isolated period. G&I method generally estimated better than other methods especially when the isolated period is 2.0 sec and design maximum displacement is relatively large. However, this method also underestimates in other conditions and have large scatteredness between each condition that reliability is not sufficient.

Despite the underestimation of the mean ratio results, standard deviation shows even results not more than the order of 0.15 in all EL methods. There no significant effects of the design maximum displacement conditions but as isolated period of the structure decreases, standard deviation also slightly decreases except for G&I method. Standard deviation of G&I method increases with the isolated period decreases except for the case u_0 is 0.1 m.

3.3 Discussions

In this chapter, five different EL methods' estimation accuracy has been evaluated. Under 20 sets of earthquake data scaled to meet various design maximum displacement variables, peak responses of displacement at base floor and peak acceleration at roof floor are derived by using equivalent linear method and nonlinear method respectively.

The results indicated that EL methods slightly overestimated the displacement of base floor except for H&C method. Especially, R&H method

and G&I method estimated accurately with error ratio less than 10 percent and small scatteredness less than standard deviation order of 0.2. It can be derived that existing EL method are quite reliable method to predict the behavior of the isolator under various earthquake excitations.

On the other hand, in the results of absolute acceleration of the roof floor, all methods estimation accuracy turns out to be significantly insufficient. EL methods underestimated the acceleration response in almost conditions except for very few cases. Despite the standard deviation of each condition is not that large, scatteredness consequential to variables' change is distributed unevenly.

Chapter 4. Analysis of Story Drift and Floor Acceleration

4.1 General

This chapter includes the floor response analysis such as absolute displacement, relative displacement, and absolute acceleration. The analysis model and earthquake data are the same as referred in previous chapter. Earthquake data is applied separately with DBE level and MCE level to reflect different aspects through data characteristics. As the capacity of this paper is limited, specific isolation conditions are selected and analyzed.

Among EL methods evaluated advanced chapter, R&H method is chosen as representative method because it is mostly adapted in current design specifications. Applied parameters of isolation system are arranged in Table 4.1 below. Normalized yield strength and post-to-pre yield stiffness ratio is 0.05 and 0.1 respectively that determined as effective value in previous subsection 3.1.3. It is also the most accepted properties of typical LRBs. Design isolated period varies from 1.5 sec to 3.0 sec with increment equal to 0.5 sec.

Table 4.1 Characteristics of isolation system

Normalized yield strength Q_y	Post-to-pre yield stiffness ratio α	Isolated period T_p (sec)
0.05	0.1	1.5
		2.0
		2.5
		3.0

4.2 Responses of Multistory Structure

DBE level earthquake response

From Figure 4.1 to Figure 4.3, the absolute displacement, relative displacement, and absolute acceleration responses on each floor are illustrated respectively when DBE level earthquake excitations occur. Analysis had been carried out with the nonlinear time history method and equivalent linear method which are differentiated by dotted line and straight line respectively. Also, distinction between target isolated period T_p is done by the line width.

It can be noted that deformation of the structure occurs almost at the base floor by Figure 4.1. Under DBE level earthquakes, isolator deforms about 0.2 – 0.3 m and with design isolated period increases, deformation of isolator increases. This is because that, as mentioned in Chapter 1, displacement of the structure is increased by increasing natural period of the structure in elastic response spectrum Figure 1.2. When it comes to the comparison of analysis methods, general deformation form is similar with two methods that error rates are almost same through all stories as indicated in Table 4.2. EL method overestimates the absolute response around 4 to 5 percent except for the case when design isolated period is 2.0 sec. In this case, EL method predicted the response with good accuracy of about 1 percent. Overall, it can be derived that EL method estimates the absolute deformation response quite well.

Figure 4.2 is the result of interstory drift that is derived by calculating the gap of each floor's absolute displacement and the upper floor's absolute displacement. The value is expressed with percent unit by dividing the gap with story height 3 m. Main interstory drifts take place at lower floor. It can be figured out that maximum floor drift occurs at second floor by nonlinear

method despite that by EL method, maximum floor drift occurs at third floor. As the design isolated period increases, floor drift decreases in both methods. In all cases, the higher floor located, the bigger error occurs. In this study, floor drift values are very small so that the error is not significant to consider, however when it comes to higher buildings over 60 m or skyscrapers, amplified interstory drift can be important matter should be considered in the design of the structure. Therefore, EL methods have to be improved to reflect the interstory drift responses at upper stories.

When it comes to consider about absolute acceleration responses, significant error occurs. As the Figure 4.3 shows, EL method generally under-estimates the absolute acceleration responses through all stories. Especially, error ratios in base floor and top floor are significantly bigger than mid floors. Maximum error occurs in the roof floor and the ratio is up to 31 percent when the design isolated period is 3.0 sec. In respect of variable change, as the design isolated period increases, not only absolute acceleration response but also the error decrease. It is explained by Figure 1.2 in that when the period shift is achieved enough by isolation system, natural period of the structure is in the range of region which is not dominated by acceleration. Considering that the average PGA of twenty earthquake data is 0.59 g, it is not appropriate to set the target-isolated period as 1.5 sec because average absolute acceleration response of roof floor is amplified over 0.7 g by nonlinear analysis. As mentioned in previous chapter, the damage of non-structural member and equipment inside the building is mostly by absolute acceleration. EL method is not proper way to estimate the response of structure from this perspective.

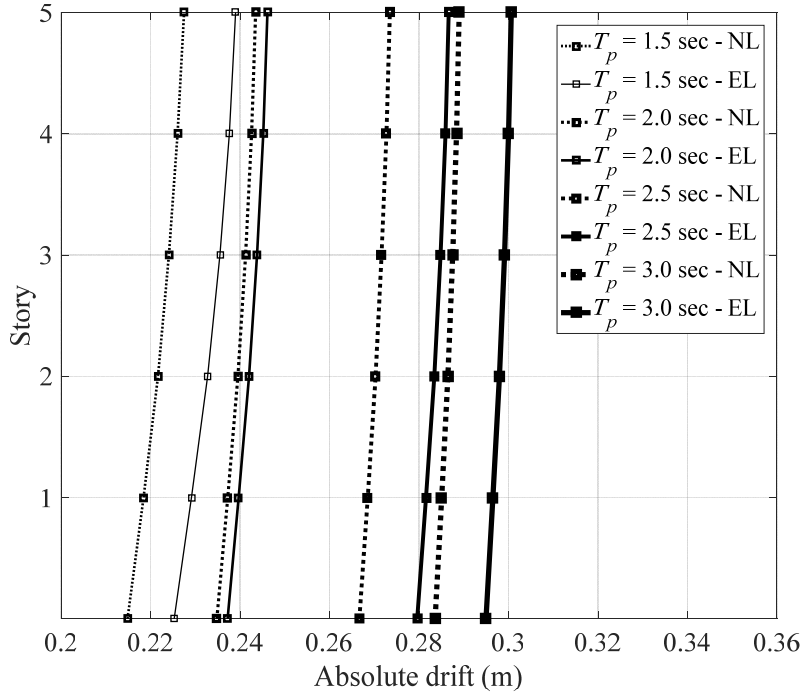

Figure 4.1 Absolute displacement response under DBE level earthquakes

Table 4.2 Comparison of absolute displacements under DBE level earthquakes

T_p (sec)	Floor	base	1	2	3	4	5
1.5	NL	0.215	0.218	0.222	0.224	0.226	0.227
	EL	0.225	0.229	0.233	0.235	0.238	0.239
	Error (%)	4.86	4.91	5.01	5.09	5.13	5.06
2.0	NL	0.235	0.237	0.239	0.241	0.243	0.243
	EL	0.237	0.240	0.242	0.244	0.245	0.246
	Error (%)	1.02	1.03	1.04	1.07	1.08	1.09
2.5	NL	0.267	0.269	0.270	0.272	0.273	0.273
	EL	0.280	0.282	0.283	0.285	0.286	0.287
	Error (%)	4.85	4.85	4.85	4.86	4.84	4.81
3.0	NL	0.284	0.285	0.286	0.288	0.288	0.289
	EL	0.295	0.297	0.298	0.299	0.300	0.301
	Error (%)	4.01	4.02	4.02	4.03	4.04	4.03

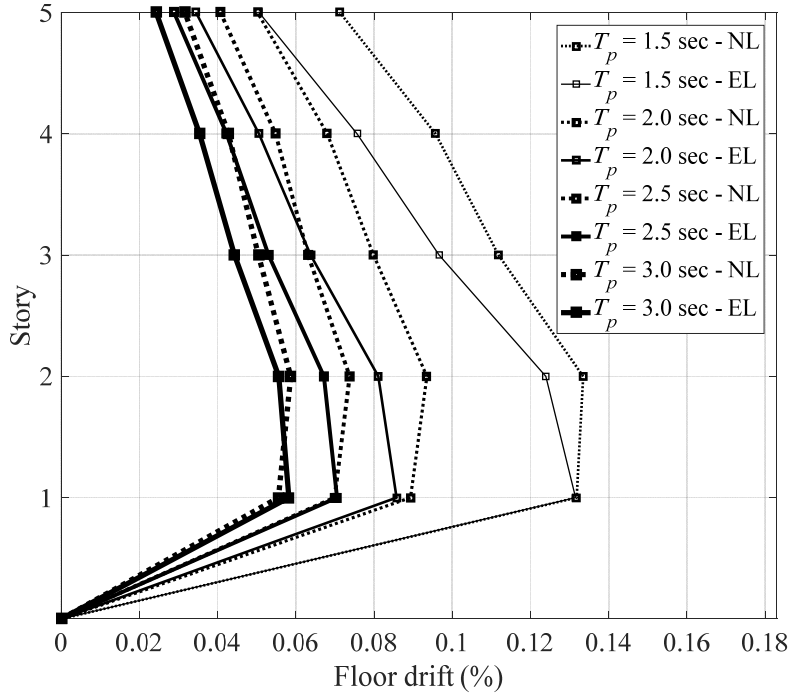

Figure 4.2 Relative displacement response under DBE level earthquakes

Table 4.3 Comparison of relative displacements under DBE level earthquakes

T_p (sec)	Floor	base	1	2	3	4	5
1.5	NL	-	0.132	0.133	0.112	0.096	0.071
	EL	-	0.132	0.124	0.097	0.076	0.051
	Error (%)	-	-0.21	-7.15	-13.57	-20.98	-29.02
2.0	NL	-	0.089	0.094	0.080	0.068	0.050
	EL	-	0.086	0.081	0.064	0.051	0.034
	Error (%)	-	-4.00	-13.27	-20.13	-25.65	-31.36
2.5	NL	-	0.070	0.074	0.063	0.055	0.041
	EL	-	0.071	0.067	0.053	0.042	0.029
	Error (%)	-	0.90	-8.95	-16.03	-22.82	-29.12
3.0	NL	-	0.056	0.059	0.050	0.043	0.032
	EL	-	0.058	0.056	0.044	0.035	0.024
	Error (%)	-	4.83	-5.22	-12.11	-17.29	-23.32

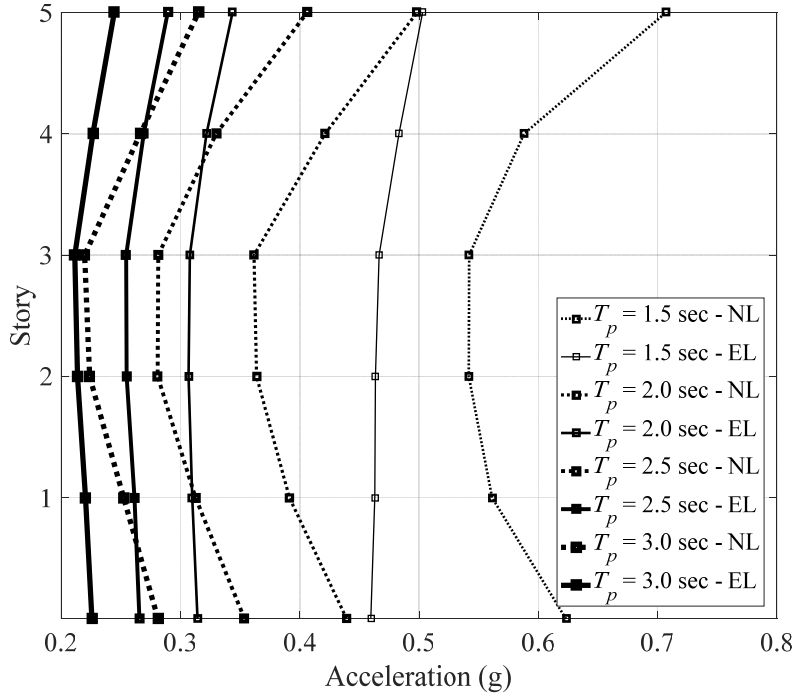

Figure 4.3 Absolute acceleration response under DBE level earthquakes

Table 4.4 Comparison of absolute accelerations under DBE level earthquakes

T_p (sec)	Floor	base	1	2	3	4	5
1.5	NL	0.62	0.56	0.54	0.54	0.59	0.71
	EL	0.46	0.46	0.46	0.47	0.48	0.50
	Error (%)	-26.26	-17.53	-14.44	-13.92	-17.85	-28.86
2.0	NL	0.44	0.39	0.36	0.36	0.42	0.50
	EL	0.31	0.31	0.31	0.31	0.32	0.34
	Error (%)	-28.47	-20.81	-15.66	-14.87	-23.61	-31.04
2.5	NL	0.35	0.31	0.28	0.28	0.33	0.41
	EL	0.27	0.26	0.25	0.25	0.27	0.29
	Error (%)	-24.90	-16.38	-9.24	-9.59	-18.42	-28.76
3.0	NL	0.28	0.25	0.22	0.22	0.27	0.32
	EL	0.23	0.22	0.21	0.21	0.23	0.24
	Error (%)	-19.73	-12.64	-4.51	-3.76	-14.94	-22.42

MCE level earthquake response

This subsection includes the results of the structure under MCE level earthquake excitations. Figure 4.4 and Table 4.5 indicate the results of absolute displacement responses. General aspects are similar but peak displacements of isolator are over 2.5 times of the responses under DBE level earthquakes. Almost all the deformation occurs in the base floor and superstructure deformation is insignificant. As the design isolated period increases, peak displacement also increases. Particularly, when design isolated period is over 2.5 sec, significant displacement over 0.7 m occurs which can bring about the damage of structural member or facilities connected through foundation to upper stories. EL method slightly overestimates the response by 4 - 6 percent.

Figure 4.5 and Table 4.6 is results of relative displacement responses on each floor. The response decreases as the design isolated period increases. It can be noticed that EL method underestimates the response compared to NL method except for the first floor of the structure. Maximum interstory drift occurs at the first floor by both of the analysis methods and the value rise dramatically compared to the increasement of absolute displacement. However, the error ratios are less than the results under DBE level earthquake excitations. On the whole, EL method seems to predict the relative displacement response of structure quite accurately.

EL method underestimates the absolute acceleration results as well. Great differences stick out at the base and roof floor just like the cases under DBE level earthquakes. Maximum errors appear on the roof floor for about 16 - 18 percent. These are somewhat smaller error ratios than results under DBE level earthquakes but still imprecise. The sharp increasement of the absolute

acceleration as the height increment is pernicious to high-rise buildings and underestimated results can incur improper design of the structure. Reminding that the average PGA of MCE level earthquakes considered in this study is 0.88 g, target isolated period over 2.5 sec seems to be acceptable.

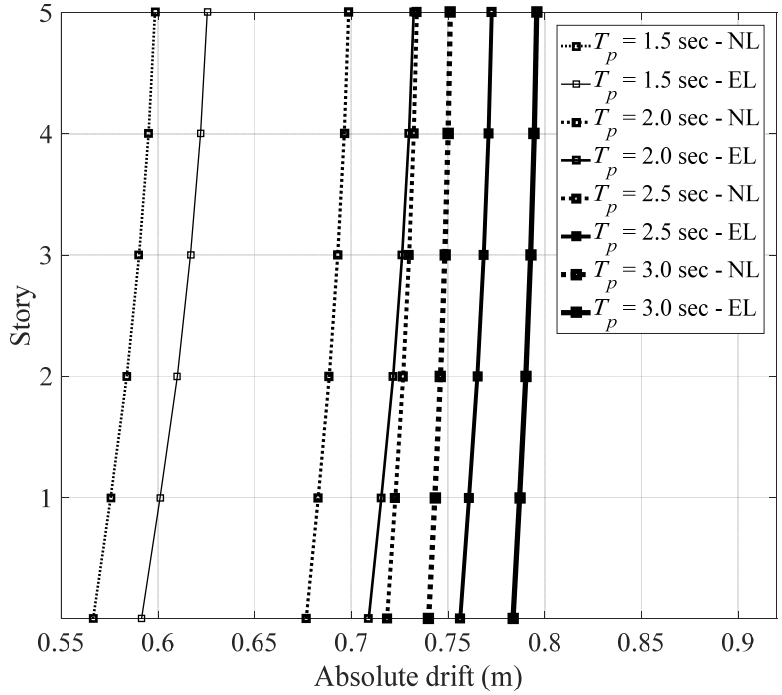

Figure 4.4 Absolute displacement response under MCE level earthquakes

Table 4.5 Comparison of absolute displacements under MCE level earthquakes

T_p (sec)	Floor	base	1	2	3	4	5
1.5	NL	0.566	0.576	0.584	0.590	0.595	0.598
	EL	0.592	0.601	0.610	0.617	0.622	0.625
	Error (%)	4.42	4.44	4.47	4.50	4.52	4.52
2.0	NL	0.677	0.683	0.689	0.693	0.696	0.699
	EL	0.709	0.715	0.722	0.726	0.730	0.732
	Error (%)	4.77	4.78	4.79	4.81	4.81	4.81
2.5	NL	0.718	0.723	0.727	0.730	0.732	0.734
	EL	0.756	0.761	0.765	0.768	0.771	0.773
	Error (%)	5.26	5.27	5.28	5.28	5.28	5.28
3.0	NL	0.740	0.743	0.746	0.748	0.750	0.751
	EL	0.784	0.787	0.790	0.793	0.795	0.796
	Error (%)	5.89	5.90	5.91	5.93	5.94	5.95

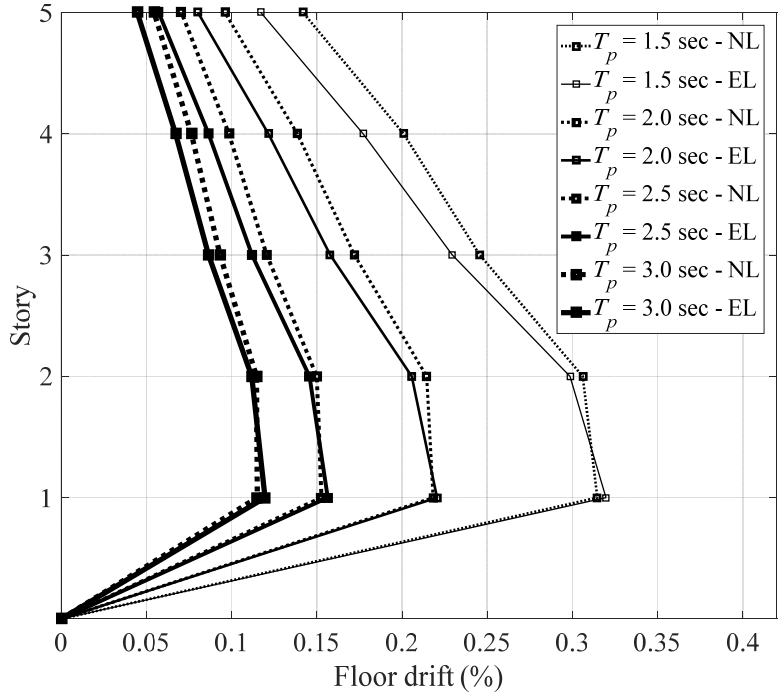

Figure 4.5 Relative displacement response under MCE level earthquakes

Table 4.6 Comparison of relative displacements under MCE level earthquakes

T_p (sec)	Floor	base	1	2	3	4	5
1.5	NL	-	0.315	0.306	0.246	0.201	0.142
	EL	-	0.320	0.299	0.230	0.177	0.117
	Error (%)	-	1.62	-2.43	-6.54	-11.80	-17.50
2.0	NL	-	0.218	0.214	0.172	0.139	0.096
	EL	-	0.221	0.206	0.158	0.122	0.080
	Error (%)	-	1.05	-4.08	-8.25	-12.22	-16.56
2.5	NL	-	0.153	0.150	0.121	0.098	0.071
	EL	-	0.156	0.146	0.112	0.086	0.057
	Error (%)	-	2.43	-2.82	-7.13	-12.10	-19.00
3.0	NL	-	0.115	0.115	0.093	0.076	0.054
	EL	-	0.120	0.112	0.086	0.067	0.045
	Error (%)	-	3.90	-2.44	-7.31	-12.09	-18.15

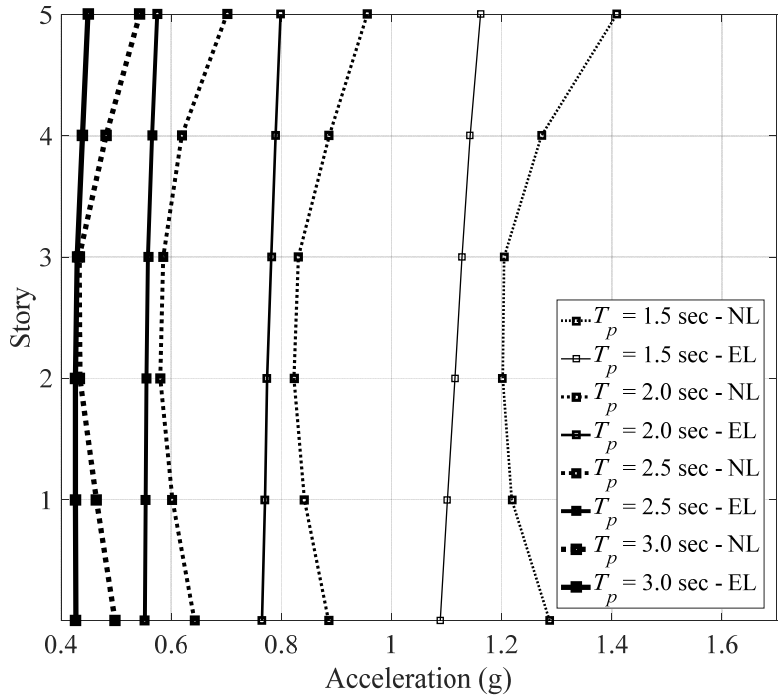

Figure 4.6 Absolute acceleration response under MCE level earthquakes

Table 4.7 Comparison of absolute accelerations under MCE level earthquakes

T_p (sec)	Floor	base	1	2	3	4	5
1.5	NL	1.29	1.22	1.20	1.20	1.27	1.41
	EL	1.09	1.10	1.12	1.13	1.14	1.16
	Error (%)	-15.45	-9.59	-7.22	-6.34	-10.19	-17.57
2.0	NL	0.89	0.84	0.82	0.83	0.89	0.96
	EL	0.76	0.77	0.77	0.78	0.79	0.80
	Error (%)	-13.67	-8.50	-5.92	-5.93	-11.00	-16.46
2.5	NL	0.64	0.60	0.58	0.59	0.62	0.70
	EL	0.55	0.55	0.55	0.56	0.57	0.57
	Error (%)	-14.06	-8.08	-4.34	-4.73	-8.70	-18.03
3.0	NL	0.50	0.46	0.43	0.43	0.48	0.54
	EL	0.43	0.43	0.43	0.43	0.44	0.45
	Error (%)	-14.31	-8.21	-1.85	-0.81	-8.91	-17.37

4.3 Detailed Analysis of Representative Examples

From the results addressed beforehand, it was recognized that EL method significantly underestimates the absolute acceleration responses of the structure under both DBE and MCE level earthquake excitations. However, previous analysis dealt with only peak value of the responses. As the earthquake excitations change from time to time and the responses can be affected by many other factors, considering only maximum value is not sufficient. In this subsection, further analysis has been accomplished with specific conditions to look through the responses of the structure over whole time. The model characteristics and isolation system properties are same as indicated in Table 4.1. Normalized yield strength ratio f is 0.05, post-to-yield stiffness ratio α is 0.1, and among the four target isolated periods considered, 2.5 sec is selected because the responses from that target period have shown quite reasonable in previous subsection. Considering the capacity limitation of the dissertation, representative case is selected to show the detailed responses for each earthquake type.

DBE level earthquake

First case is the responses under Imperial Valley (1979) which is scaled to meet DBE level design spectrum at California region. The magnitude of the earthquake is 6.5 and peak ground acceleration is 0.49 g. The distance from the epicenter is only 4.1 km which means the earthquake is critical excitation. Figure 4.8 shows the time history data of the earthquake acceleration. It can be noticed during the whole time excitation of 40 seconds, strong motion duration lasts until 10 sec which means the isolator is triggered at this region and behaves

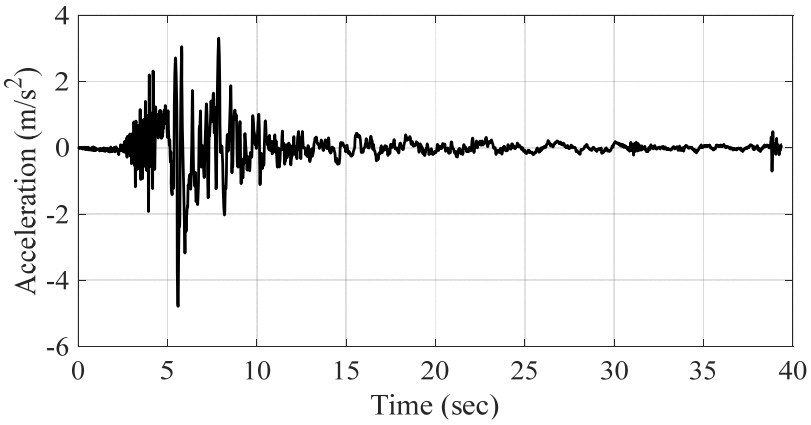

Figure 4.8 Time history acceleration of Imperial Valley Earthquake

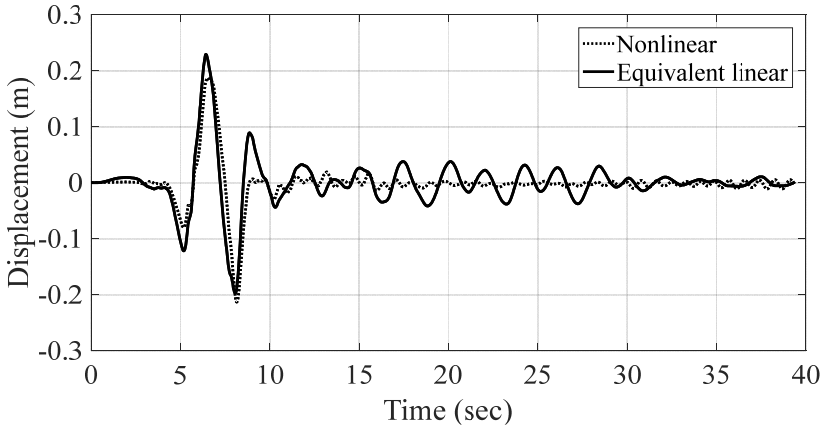

Figure 4.9 Relative displacement response of base floor

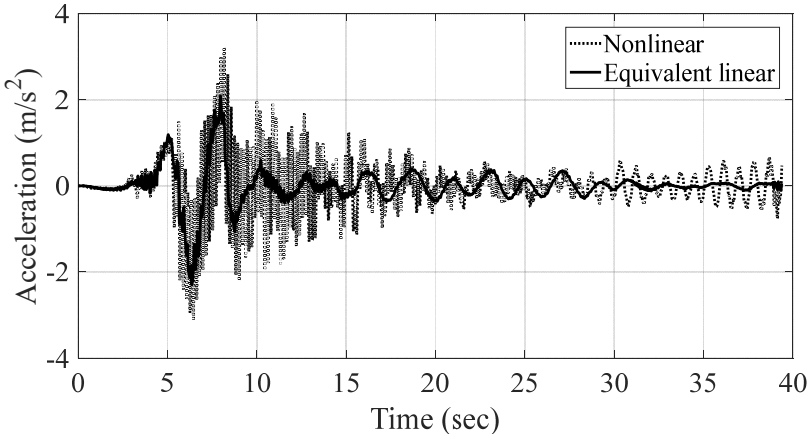

Figure 4.7 Absolute acceleration response of roof floor – time domain

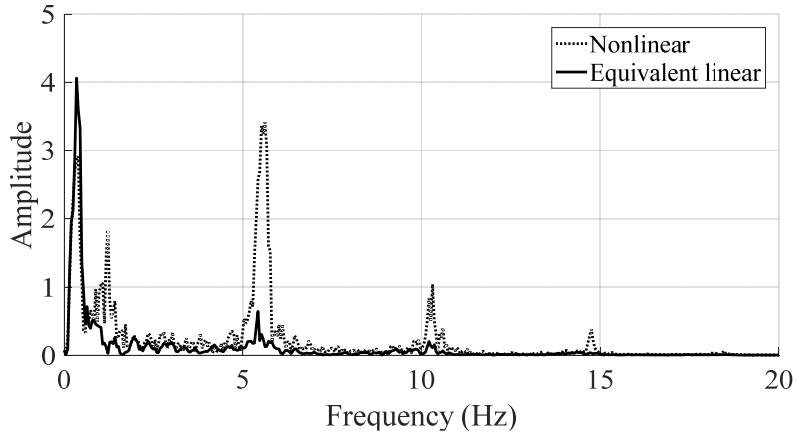

Figure 4.10 Absolute acceleration response of roof floor – frequency domain

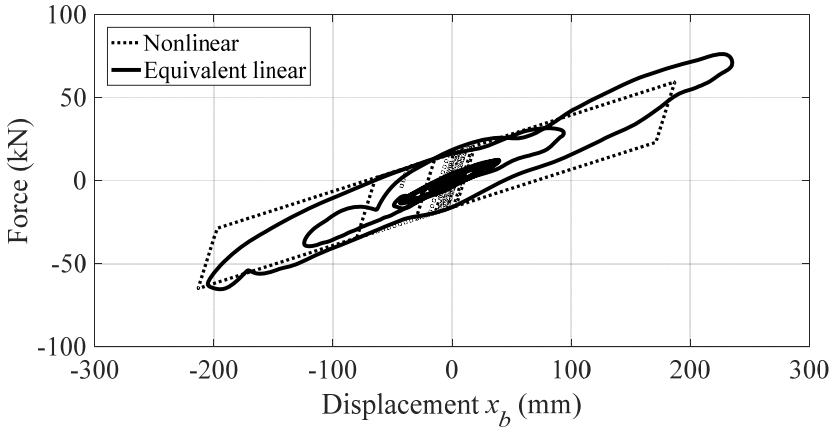

Figure 4.11 Hysteresis loop of isolator

as bilinear hysteresis. After the strong motion duration passed, isolator and superstructure moves in free vibration motion until the earthquake ends.

Relative displacement at base floor, absolute acceleration at roof floor in time domain and frequency domain, hysteresis loop of isolator responses are arranged in regular sequence through Figure 4.9 to Figure 4.11. As reported in previous section, EL method slightly overestimates the peak relative displacement response of base floor with the value of 0.23 m when the peak

relative displacement from NL method is 0.21 m. In the point of the time domain response, in the strong motion duration section, NL and EL method responses are quite similar with each other. However, in the free vibration section, result from EL method behaves based on the target period of the isolator despite result from NL method includes the high frequency. From the Figure 4.7 which indicates absolute acceleration response of roof floor, EL method underestimates the response over the time. The value of peak absolute acceleration by NL and EL method are 0.33 g and 0.24 g respectively. Especially, the gap is significantly large in the free vibration section.

The justification of the error can be found in the Figure 4.10 which indicates the frequency domain response of the structure. EL method reveals the response frequency of 0.25 Hz dominantly which is relevant to the target period 2.5 sec and there is no significant response in other frequency range. On the other hand, from the NL method, there are additional frequency range that the structure responded. One of the dominant response is activated at the frequency of the isolator and the other is at the frequency that reflects the structure behavior. By considering the amplitude of the acceleration, structure behavior has influence fairly. Especially, this influence is because that under DBE level earthquake, the portion of elastic behavior prior to the isolator activation is pretty considerable. This phenomenon is also explained by the hysteresis loop of isolator (Figure 4.11). Note that Y-axis of the Figure 4.11 is the sum of the elastic restoring force and damping force of the isolator and X-axis means the trace of the isolator movement. The value of ductility ratio μ is 27.5 which means that isolator behaves significantly after the yield point. The loop of EL method shows that the isolator behaves mainly through the line that connects the maximum displacement and starting point.

MCE level earthquake

Representative case of the MCE level earthquake is Kobe earthquake (1995). The magnitude is 6.9, PGA value is 0.92 g, and distance from the epicenter is 3.4 km, which is significantly strong excitation occurred in Japan. From the shape of the earthquake shown in Figure 4.13, extremely strong impact came out firstly, and free vibration is followed after another strong motion around 12 sec.

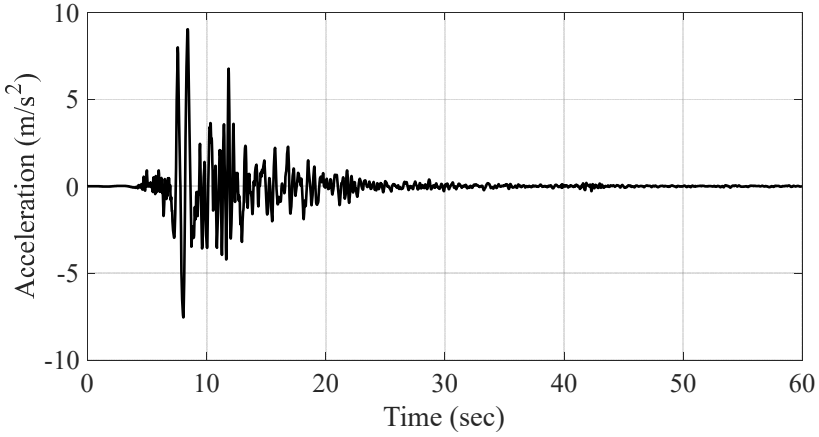

Figure 4.13 Time history acceleration of Kobe earthquake

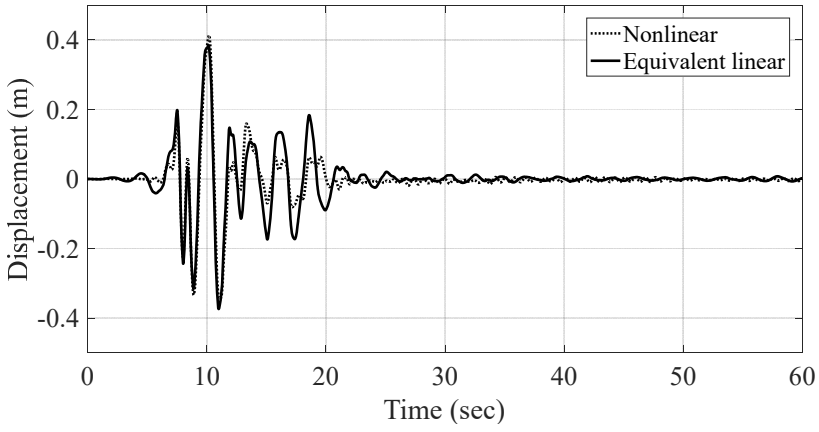

Figure 4.12 Relative displacement response of base floor

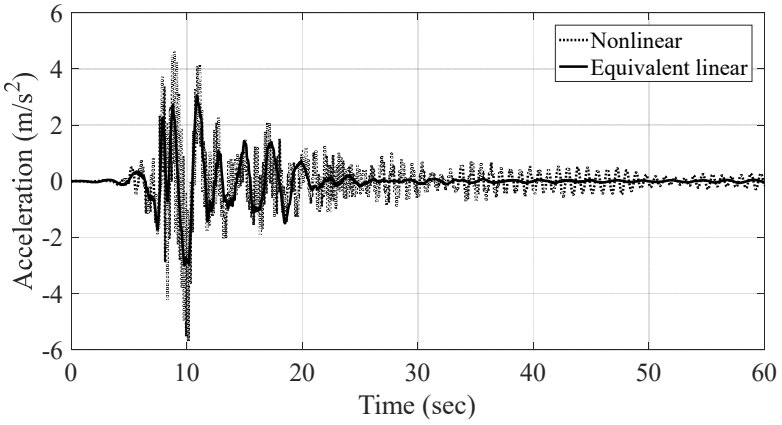

Figure 4.14 Absolute acceleration response of roof floor – time domain

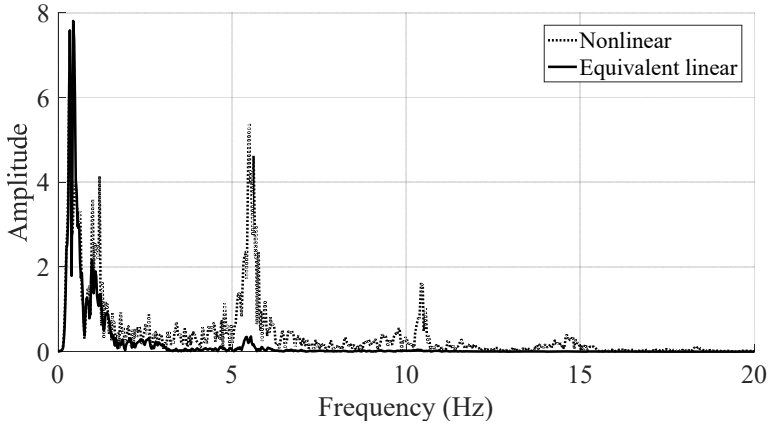

Figure 4.15 Absolute acceleration response of roof floor – frequency domain

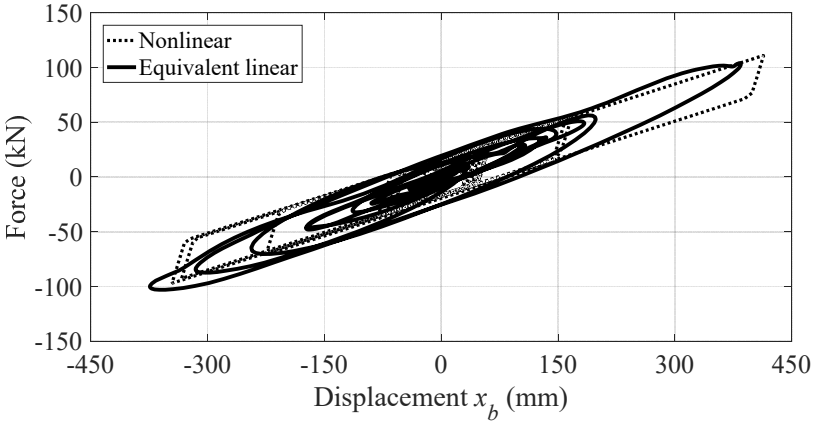

Figure 4.16 Hysteresis loop of isolator

Figure 4.12 shows that the nonlinear analysis and equivalent linear analysis estimate the relative displacement response of the base floor quite similarly. In this case, the peak deformation of base floor from the nonlinear analysis is larger than that from the equivalent linear analysis. The maximum displacement is up to 400 mm. It can also be noticed that after the strong motion duration, the response from EL analysis expresses the shape that sloshing with specific low frequency. On the other hand, response of nonlinear analysis includes additional frequency contents.

When it comes to absolute acceleration response of roof floor, EL method significantly underestimates the response compared to the NL method. From the Figure 4.14, while the peak acceleration from the nonlinear analysis is up to 0.59 g, peak acceleration response from the equivalent linear analysis is about 0.33 g which means that the estimation accuracy error is up to 44 %. Moreover, the range of frequency that is included in the response from EL method is relatively narrow. This result can be also analyzed by Figure 4.15. In this figure, NL method includes several dominate frequencies that lead quite high amplitudes. However, EL method includes only the frequency of the target frequency of the isolated structure with neglecting the other frequency ranges. Compared to the results of the DBE level earthquake case, the Imperial Valley (1979), the response of the target frequency is more sticked out. It is explained by the hysteresis loop of isolator. Under the MCE level earthquake, the isolator activated more easily and moves through the nonlinear behavior. So the influence of the equivalent stiffness gets much larger.

4.4 Discussion

In this chapter, floor responses were carried out under the DBE and MCE level earthquake excitations respectively. Results indicate the there are some different aspects between the result from the NL method and that from the EL method. Despite the absolute displacement responses and relative displacement of the floor responses show the similar results with quite acceptable error, absolute acceleration responses turn out to have significantly underestimated by the EL method. Especially, the error is even larger in the lower and upper floors of the structure. The absolute acceleration is the index that indicates the damage of the non-structural elements and the equipment.

Further analysis was done to look through not only the peak responses but also the responses through the whole time excitation. With the generally used properties of the LRBs, time history analysis was carried out. From the results, it was found that in the strong motion duration, the responses estimation from the NL and EL methods are quite similar. However, when it comes to free vibration duration, significant estimation error is occurred. Despite the responses from the nonlinear analysis includes broad-band frequencies, EL method's responses behaves mainly by the target period of the isolator.

As mentioned in chapter 3, the absolute acceleration responses are significantly underestimated with the EL method not only for the peak value but also for the whole time of the earthquake excitation. Moreover, acceleration responses from the EL method include less frequency range than that from the NL method. By arranging the acceleration response by the frequency domain, it was clearly expressed that EL method consider the frequency of the isolator mostly and almost neglect the other frequency response ranges.

Chapter 5. Conclusions

In this paper, the evaluation of the equivalent linear method was implemented by analyse the responses about the structure characterized with multi-degree-of-freedom by nonlinear and equivalent linear methods. The analysis results include the evaluation of the EL methods and the aspects of the responses of each floor. The summary of this study is written below.

Time history analysis of seismically isolated 5 story building has been done by nonlinear (NL) and equivalent linear (EL) method respectively. Relative displacement and absolute acceleration were taken as indicators to investigate the damage of structural and non-structural member respectively.

Several EL methods - Rosenblueth and Herrera, Dicleli and Buddaram, Guyader and Iwan - estimate the relative displacement of the base floor response almost accurately with the error ratio less than 5 percent when the isolator properties are adjusted ordinarily. Relative displacement is important index that affects the structural damage, so that EL method is considered to be reliable analysis method in the preliminary design of the structure.

Absolute acceleration response turned out to underestimate the superstructure's behavior significantly in all EL methods. Especially, the error is larger in upper and lower floors. It means that EL method cannot include the non-structural damage and required performance of the structure.

The reason of the error is that EL method cannot reflect the structure mode unlike the nonlinear method. EL method dominantly moves with the target frequency and other frequency elements are almost ignored.

Given that the EL method is the subsidiary design method and used as initial design, this method is significantly acceptable for the relative displacement response. However, as most of the damage in the low-to-mid earthquake hazard region occurs by failure of non-structural elements and breakdown of equipment, further research about the EL method that considers both isolation mode and the structure mode is required.

References

Bridgestone: Figures of natural rubber bearings and lead-rubber bearings <http://www.bridgestone.com/products/>

Chopra, A. K. (1995). Dynamics of structures, Prentice Hall New Jersey.

Chimamphant, S. and K. Kasai (2016). "Comparative response and performance of base-isolated and fixed-base structures." Earthquake engineering & structural dynamics 45(1): 5-27.

Christopoulos, C., et al. (2006). Principles of passive supplemental damping and seismic isolation, Iuss press.

Dicleli, M. and S. Buddaram (2007). "Comprehensive evaluation of equivalent linear analysis method for seismic-isolated structures represented by sdof systems." Engineering Structures 29(8): 1653-1663.

Gulkan, P. and M. A. Sozen (1974). Inelastic responses of reinforced concrete structure to earthquake motions. ACI Journal Proceedings, ACI.

Guyader, A. and W. Iwan (2004). An improved capacity spectrum method employing statistically optimized linearization parameters. Proceedings of the 13th world conference on earthquake engineering, Vancouver, Canada.

Guyader, A. C. and W. D. Iwan (2006). "Determining equivalent linear parameters for use in a capacity spectrum method of analysis." Journal of Structural Engineering 132(1): 59-67.

Hwang, J. and J. Chiou (1996). "An equivalent linear model of lead-rubber seismic isolation bearings." Engineering Structures 18(7): 528-536.

Hwang, J. and L. Sheng (1993). "Effective stiffness and equivalent damping of base-isolated bridges." Journal of Structural Engineering 119(10): 3094-3101.

Iwan, W. (1980). "Estimating inelastic response spectra from elastic spectra." Earthquake engineering & structural dynamics 8(4): 375-388.

Iwan, W. D. and N. C. Gates (1979). "Estimating earthquake response of simple hysteretic structures." Journal of the Engineering Mechanics Division 105(3): 391-405.

Jangid, R. and J. Kelly (2001). "Base isolation for near-fault motions." Earthquake engineering & structural dynamics 30(5): 691-707.

Jara, M. and J. R. Casas (2006). "A direct displacement-based method for the seismic design of bridges on bi-linear isolation devices." Engineering Structures 28(6): 869-879.

Jara, M., et al. (2012). "Improved procedure for equivalent linearization of bridges supported on hysteretic isolators." Engineering Structures 35: 99-106.

Kelly, J. and S. Hodder (1982). "Experimental study of lead and elastomeric dampers for base isolation systems in laminated neoprene bearings." Bulletin of the New Zealand National Society for Earthquake Engineering 15(2): 53-67.

Kelly, J., et al. (1987). "Robust control of base-isolated structures under earthquake excitation." Journal of Optimization Theory and Applications 53(2): 159-180.

Kelly, J. M. (1993). Earthquake-resistant design with rubber, Springer.

Kelly, J. M. (1999). "The role of damping in seismic isolation." Earthquake engineering & structural dynamics 28(1): 3-20.

Kelly, J. M. and H. C. Tsai (1985). "Seismic response of light internal equipment in base-isolated structures." Earthquake engineering & structural dynamics 13(6): 711-732.

Kwan, W.-P. and S. L. Billington (2003). "Influence of hysteretic behavior on equivalent period and damping of structural systems." Journal of Structural Engineering 129(5): 576-585.

Liu, T. (2014). Equivalent Linearization Analysis Method for Base-isolated Buildings, University of Trento.

Liu, T., et al. (2014). "Evaluation of equivalent linearization analysis methods for seismically isolated buildings characterized by SDOF systems." Engineering Structures 59: 619-634.

Liu, T., et al. (2014). "An improved equivalent linear model of seismic isolation system with bilinear behavior." Engineering Structures 61: 113-126.

Makris, N. and G. Kampas (2013). "The engineering merit of the 'effective period'of bilinear isolation systems." Earthquakes and Structures 4(4): 397-428.

Makris, N. and G. Kampas (2013). "The engineering merit of the "effective period" of bilinear isolation systems." Earthquakes and Structures 4(4): 397-428.

MATLAB R2016a [Computer software]. MathWorks, Natick, MA.

Maurer: Figure of friction pendulum system < http://www.maurer.eu/>

Nagarajaiah, S. and S. Xiaohong (2000). "Response of base-isolated USC hospital building in Northridge earthquake." Journal of Structural Engineering 126(10): 1177-1186.

Oiles: Figure of basic characteristics of friction pendulum system <http://www.oiles.co.jp/en/menshin/building/menshin/products/>

Prayag J. Sayani; Keri L. Ryan, M. A. (2009). "Comparative Evaluation of Base-Isolated and Fixed-Base Buildings Using a Comprehensive Response Index." Journal of Structural Engineering 135(6): 698-707.

Ramallo, J., et al. (2002). ""Smart" base isolation systems." Journal of Engineering Mechanics 128(10): 1088-1099.

Rosenblueth, E. and I. Herrera (1964). "On a kind of hysteretic damping." Journal of the Engineering Mechanics Division 90(4): 37-48.

Skinner, R. I., et al. (1993). An introduction to seismic isolation, John Wiley & Sons.

Somerville, P. G. and S. J. Venture (1997). Development of ground motion time histories for phase 2 of the FEMA/SAC steel project, SAC Joint Venture.

Tjhin, T., et al. (2005). "Estimates of peak roof displacement using “equivalent” single degree of freedom systems." Journal of Structural Engineering 131(3): 517-522.

Zhang, T. L. T. Z. Q. (2015). "Equivalent Viscous Damping of Bilinear Hysteretic Oscillators." Journal of Structural Engineering 141(11): 06015002.

Zordan, T., et al. (2014). "Improved equivalent viscous damping model for base-isolated structures with lead rubber bearings." Engineering Structures 75: 340-352.

Appendix A

Requirements in modifying nonlinear behavior to equivalent linear behavior

Many specifications that allow of using equivalent linear behavior as isolators' hysteresis, nonlinear behavior of seismic isolation system may be considered as being equivalent linear only if all the following requirements are satisfied.

(1) The equivalent stiffness, Keq, should be greater or equal to 50% of the secant stiffness for cycles with displacement equal to 20% of the design displacement, as shown in Figure A.1, namely

$$\frac{k_{eq}}{k_{0.2eq}} = \begin{cases} \dfrac{1+\alpha(\mu-1)}{\mu}\dfrac{0.2\mu}{1+\alpha(0.2\mu-1)} & \text{if} \quad \mu \geq 5 \\ \dfrac{1+\alpha(\mu-1)}{\mu} & \text{if} \quad \mu < 5 \end{cases} \geq \frac{1}{2}$$

Simplifying the above inequality, the relationship between μ and α can be derived in order to satisfy this requirement, which can be expressed as

$$\begin{cases} \mu \geq \max\left(\dfrac{3(1-\alpha)}{\alpha}, 5\right) \\ \mu < \min\left(\dfrac{2(1-\alpha)}{1-2\alpha}, 5\right) \end{cases}$$

However, considering the maximum post-to-pre yield stiffness ratio α = 0.2 and the second item of equation 0.0, the ductility ratio has to be less than 2.67 which is not suitable for seismic isolation subjected to design earthquakes.

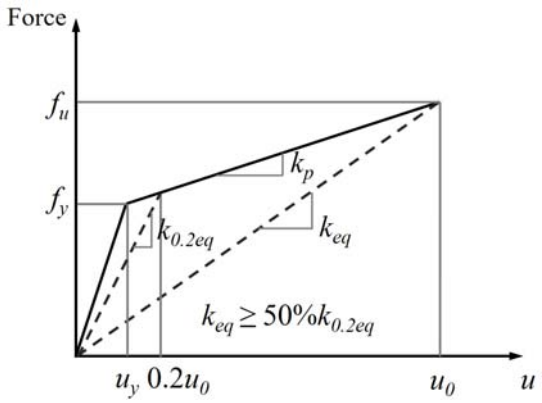

Figure A.1 Requirement of equivalent stiffness in linearization of bilinear behavior

(2) The equivalent damping ratio, ξeq, of seismic isolation system should be less than 30%, that is

$$\xi_{eq} = \xi_0 + \frac{2(1-\alpha)(\mu-1)}{\pi\mu\left[1+\alpha(\mu-1)\right]} \leq 0.30$$

(3) The force-displacement characteristics of seismic isolation system do not vary more than 10% due to the rate of loading and the variation of vertical load. In order to simplify the assessment of the procedure, the force-displacement characteristics of isolation system are assumed to be independent of the above aspects in this study.

(4) To provide sufficient re-centering capability, increase of the force in isolation system for displacements between $0.5u_0$ and u_0 is not less than 2.5% of the total gravity load above the system, as presented in Figure A.2.

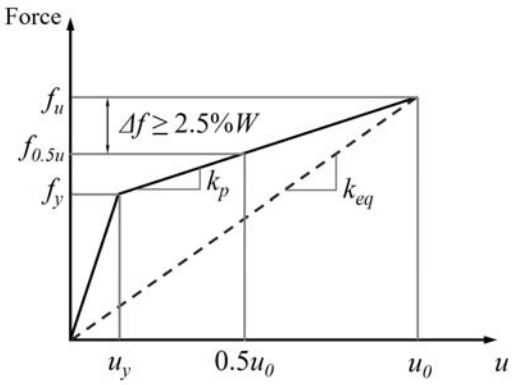

Figure A.2 Requirement of restoring force in linearization of bilinear behavior

국 문 초 록

면진은 상부구조물과 기초 사이에 횡강성이 낮은 면진장치 도입을 통해 대부분의 변형을 면진장치에 집중시키고, 구조물에 가해지는 지진력을 소산함으로써 구조물의 피해를 저감시키는 시스템이다. 면진이 적용된 구조물은 일반적으로 상부구조물이 강체처럼 작용하여 단자유도 구조물로 단순화하여 해석한다. 또한, 면진장치는 실제로 복잡한 비선형 이력거동을 나타내지만 면진에 주로 사용되는 마찰진자 (Friction pendulum), 고무적층받침 (Laminated-rubber bearing), 납-고무적층받침 (Lead-rubber bearing) 의 경우 이러한 복잡한 비선형 거동을 이선형 모델로 단순화한다. IBC 2015, FEMA-440, Eurocode 8을 포함한 구조기준은 제한된 지진 규모와 지반조건 등을 만족하는 경우에 대해 비선형 이력거동과 같은 에너지를 소산하는 등가강성과 등가점성감쇠로 나타낼 수 있는 등가선형 모델의 사용을 허용하고 있다. 조건을 만족하지 않는 경우에 대해서도 기초 설계 과정에서 등가선형방식이 사용된다.

본 연구에서는 납-적층고무받침 (Lead-rubber bearing)이 적용된 다자유도 구조물에 대하여, 지금까지 연구되어 온 등가선형

모델의 정확성 평가를 수행하였다. 먼저, 항복 전 대비 항복 후 강성비와 면진된 구조물의 주기를 변수로 하여 여러 설계코드에서 제한하는 영역을 벗어나 다양한 변위연성도를 갖는 경우에 대해 해석을 수행하였다. 적용 지진파는 FEMA에서 제공하는 20가지 지진파를 x, y 방향으로 나눈 총 40개의 입력지진기록을 사용하였다. 등가선형모델은 이론적 또는 해석적으로 도출된 5가지 모델에 대해 해석을 수행하였다.

해석 결과 구조부재의 피해에 영향을 주는 면진장치의 최대 변형의 경우, Hwang and Chiou 모델을 제외한 등가선형 모델이 구조물 응답을 상당히 정확하게 예측하는 것을 확인하였다. 특히, Rosenblueth and Herrera 모델과 Guyader and Iwan 모델의 경우 면진장치의 최대 변형 오차율이 5% 이내로 나타나 등가선형 모델의 높은 신뢰성을 확인하였다. 하지만 비구조재나 설비 장치의 성능에 영향을 주는 절대 가속도 응답에서는 등가선형모델에 의한 해석 결과가 비선형 해석 결과에 비해 상당히 과소평가하는 것으로 나타났다. 또한 다자유도 구조물의 상부 층에서 비선형 해석과 등가선형 해석의 오차가 더욱 커짐을 확인하였다. 따라서 주파수 변환을 통한 원인을 분석했고, 등가선형모델이 면진된 구조물에 대해 구조 모드 응답을 반영하지 않음을 확인했다. 따라서 향후 면진장치의 최대변형뿐 아니라 비구조재의 피해를 나타내는 절대 가속도 응답을 고려하여 발전된 형식의 등가선형모델 개발이 요구된다.

주요어 : 내진, 면진시스템, 비선형동적해석, 등가선형해석, 납-고무적층받침

학번 : 2015-21097